The pleiotropic effects of prebiotic galacto-oligosaccharides on the aging gut

Jason W Arnold
University of North Carolina at Chapel Hill
Jeffery Roach
University of North Carolina at Chapel Hill
Salvador Fabela
University of North Carolina at Chapel Hill
Emily Moorfield
University of North Carolina at Chapel Hill
Shengli Ding
University of North Carolina at Chapel Hill
Eric Blue
University of North Carolina at Chapel Hill
Suzanne Dagher
North Carolina State University
Scott Magness
University of North Carolina at Chapel Hill
Rita Tamayo
University of North Carolina at Chapel Hill
Jose Bruno-Barcena
North Carolina State University
M. Andrea Azcarate-Peril (azcarate@med.unc.edu)
University of North Carolina at Chapel Hill https://orcid.org/0000-0003-0325-1289

Research

Keywords: Gut Microbiome, Prebiotics, Bifidobacterium, Intestinal Permeability, Host- Microbiota Interactions, Diet, Antibiotics, Metagenomics, Transcriptomics, Organoids

Posted Date: February 24th, 2020

DOI: https://doi.org/10.21203/rs.2.24333/v1

Version of Record: A version of this preprint was published at Microbiome on January 28th, 2021. See the published version at https://doi.org/10.1186/s40168-020-00980-0.

The pleiotropic effects of prebiotic galacto-oligosaccharides on the aging gut

Jason W. Arnold[1], Jeffery Roach[2], Salvador Fabela[1#], Emily Moorfield[3], Shengli Ding[3], Eric Blue[3], Suzanne Dagher[6], Scott Magness[4], Rita Tamayo[5], Jose M. Bruno-Barcena[6], and M. Andrea Azcarate-Peril[1*]

[1] Department of Medicine, Division of Gastroenterology and Hepatology, and UNC Microbiome Core, Center for Gastrointestinal Biology and Disease, School of Medicine, University of North Carolina, Chapel Hill, NC

[2] Research Computing, University of North Carolina, Chapel Hill, NC

[3] Department of Cell Biology and Physiology, University of North Carolina, Chapel Hill, NC

[4]Department of Biomedical Engineering, University of North Carolina, Chapel Hill, NC and North Carolina State University, Raleigh, NC.

[5] Department of Microbiology and Immunology, University of North Carolina, Chapel Hill, NC

[6] Department of Plant and Microbial Biology, North Carolina State University, Raleigh, NC

[#]Current affiliation: Programa de Inmunología Molecular Microbiana. Departamento de Microbiología y Parasitología, Facultad de Medicina, Universidad Nacional Autónoma de Mexico, Mexico.

*To whom correspondence should be addressed:

Department of Medicine

332 Isaac Taylor Hall - Campus Box 7555

School of Medicine

University of North Carolina

Chapel Hill, NC 27599-7545

Email: azcarate@med.unc.edu

Abstract

Background: Prebiotic galacto-oligosaccharides (GOS) have an extensively demonstrated beneficial impact on intestinal health. In this study, we determined the mechanistic impact of GOS diets on hallmarks of gut aging: microbiome dysbiosis, inflammation, and intestinal barrier defects ("leaky gut"). We also evaluated if short-term GOS feeding influenced how the aging gut responded to antibiotic challenges, since these interventions are common and relevant in older adults. Finally, we assessed the ability of colonic organoids to reproduce *in vivo* responses to GOS.

Results: Old animals had a distinct microbiome characterized by lower diversity, increased ratios of non-saccharolytic *versus* saccharolytic bacteria and lower abundance of O-Glycosyl hydrolases. GOS treatment increased abundance of non-saccharolytic (*Akkermansia muciniphila*) and saccharolytic bacteria (species of *Bacteroides* and *Lactobacillus*), and increased the abundance of β-galactosidases and β-glucosidases in young and old animals. Clyndamicin treatment reduced the abundance of beneficial bacteria including *Bifidobacterium* and *Lactobacillus*, while increasing *Akkermansia, Clostridium, Coprococcus, Enterococcus, Bacillus, Bacteroides,* and *Paenibacillus*. Prebiotics impacted the effects of the antibiotics decreasing the abundance of *Akkermansia* in the GOS-antibiotic groups compared to the control-antibiotics groups.

GOS reduced the age-associated increased intestinal permeability via increased *MUC2* expression and mucus biosynthesis. Transcriptomics analysis of colon from old animals fed GOS diets showed increased expression of genes involved in small molecule metabolic processes and specifically the respirasome, which could indicate an increased oxidative metabolism and energetic efficiency. In young mice, GOS induced expression of binding-related genes and the galectin gene *Lgals1*, a β-galactosyl-binding lectin that bridges molecules by their sugar moieties, forming a signaling and adhesion network. Further analysis showed higher

expression levels of genes in focal adhesion, PI3K-Akt and ECM-receptor interaction pathways. GOS reduced the expression of TNFα in old animals, and altered serum levels of inflammatory biomarkers IL-6, IL-17, IP-10 and Eotaxin. Stools from young mice exhibiting variable bifidogenic response to GOS, injected into colon organoids in the presence of prebiotics, reproduced the response and non-response phenotypes.

Conclusions: GOS modulation of intestinal homeostasis likely occurs through direct GOS-host interactions via modulation of host gene expression and mucus production, as well as through interactions mediated by the gut microbiota that result in increased or restored saccharolytic potential.

Keywords: Gut Microbiome, Prebiotics, *Bifidobacterium*, Intestinal Permeability, Host-Microbiota Interactions, Diet, Antibiotics, Metagenomics, Transcriptomics, Organoids.

Background

The fragility of the gut microbiota and consequent susceptibility to disease are accentuated at the beginning and at the end of life. The aging gut microbiome has a demonstrated altered bacterial diversity with reductions in the abundance of beneficial microorganisms [1-12]. Imbalances in the gut microbiota promote a basal inflammatory state and enhance susceptibility to viral and bacterial infections, including *Clostridioides difficile* [13-15]. The elderly human gut microbiome has been reported to have reduced abundance of *Bifidobacterium*, *Faecalibacterium prausnitzii* and *Clostridium* XIVa [2-4] and increased *Clostridium perfringens*, coliforms, enterococci [1], *Streptococcus, Staphylococcus,* and *Enterobacteria* [2, 3, 5-7]. Accordingly, the aging human gut microbiota shows a loss of genes involved in the production of short chain fatty acids (SCFAs) and a decrease in saccharolytic potential, with reduced representation of starch, sucrose, galactose, glycolysis and gluconeogenesis metabolism pathways, a concomitant loss of fibrolytic microorganisms and an overall increase in proteolytic function [16]. Consistent with human microbiome observations, old mice have a distinctive gut microbiome characterized by lower phylogenetic diversity, increased representation of potentially pathogenic taxa including *Rikenella* and *Enterobacteriaceae*, and reduced representation of di-, oligo-, and polysaccharide utilization genes [17].

The ability of bacteria to access host tissues is limited by the mucus layer in healthy individuals. In mice, the colon of old animals has a thinner firm mucus layer (<10 μm) compared to young mice (20–25 μm), resulting in a failure to spatially compartmentalize the microbiota to the intestinal lumen [18, 19]. The number of mucus-producing goblet cells does not decline in specialized follicle-associated epithelium in aged mice [20]. The mucus protein composition is relatively homogeneous along the intestine; however, the main mucin component synthesized and secreted by intestinal goblet cells, MUC2, shows region specific O-glycan patterns [21, 22].

Expression and secretion of MUC2 is modulated by the microbiota in part by induction of mucin production [22]. Moreover, changes in properties of the mucus barrier are associated with shifts in bacterial community composition [23]. For example the beneficial microorganisms *Lactobacillus plantarum* [24] and *Akkermansia muciniphila* [25] have been shown to promote an increase in mucus thickness and improve host tight junctions in aging animals, reducing permeability. Likewise, *Bifidobacterium* provides protection against deterioration of the colonic mucus layer, counteracting negative influences of Western diets on mucin production and hyper-degradation by enhancing production, but the mechanisms by which this phenomenon occurs is largely undiscovered [26, 27].

An increased inflammatory state is another hallmark of gut aging [28]. Aging changes the balance between inflammatory and anti-inflammatory cytokines favoring an excessive production of IL-6, TNFα, and IL-1β, directly affecting intestinal permeability [28, 29]. Traditionally, immuno-senescence, which is a decrease in the efficiency of the immune system over time, has been considered the largest contributor to increases in inflammatory mediators [30, 31]. However, recent studies have highlighted a prominent role of dysbiotic states of the gut microbiota in inflammatory bowel conditions and metabolic diseases [32, 33], which show age-related increases in incidence [34].

Prebiotic β(1-4) galacto-oligosaccharides (GOS) are complex carbohydrates that are resistant to digestion in the upper gastrointestinal tract. GOS arrives at the colon intact and consequently increase the abundance of specific primary and secondary degraders, resulting in an expanded probiome (beneficial members of the intestinal microbiota) [35]. GOS and fructo-oligosaccharides are the preferred prebiotics currently added to commercial infant formula to mimic the beneficial effects of the human milk oligosaccharides (HMOs) in breast milk [36]. Akkerman et al. [37] recently reviewed the effects of non-digestible carbohydrates in infant formulas as substituents of HMOs on the gut microbiota and maturation. They state that,

beyond a well-established role in bifidogenesis, GOS also act as soluble decoy receptors to prevent adhesion of pathogens to epithelial cells, stimulate tight junctions and enhance intestinal barrier function through modulation of goblet cells [38], and reduce the release of the inflammatory marker CXCL8 by Caco-2 cells [39]. In addition, GOS support intestinal development in piglets, increasing expression levels of β-defensins-2 and sIgA, suggesting improvement of mucosal immune responses [40]. In adults, increases in the abundance of *Bifidobacterium* upon GOS consumption have been reported in humans and animal models [41-45]. We demonstrated that specific bifidobacteria (*B. longum, B. adolescentis, B. catenulatum,* and *B. breve*) increased when lactose-intolerant adults received purified GOS [46, 47]. We also demonstrated that pure GOS are capable of increasing the abundance of beneficial bacteria including *Faecalibacterium prausnitzii,* and species of *Lactobacillus*, *Christensenellaceae*, *Collinsella*, *Prevotella,* and *Catenibacterium* [45, 47]. In addition, GOS directly induce expression of *MUC2, TFF3* and *RETNLB* in the colonic adenocarcinoma LS174T cell line, which exhibits a goblet cell-like phenotype [38]. Finally, studies in humans showed that GOS significantly increased the numbers of bifidobacteria, phagocytosis, NK cell activity, and anti-inflammatory IL-10 in healthy elderly individuals, with a significant reduction in the production of proinflammatory cytokines (IL-6, IL-1β, and tumor necrosis factor-α) [48].

Based on the demonstrated effects of GOS on infants and adults, our study aimed to determine the mechanistic impact of pure GOS [49] on hallmarks of gut aging. We also further evaluated the effect of short-term GOS feeding on how the aging gut microbiome responds to antibiotic challenges, since these interventions are common and relevant in older adults. In fact, in the years 2007 to 2009, patients aged ≥65 years used more antimicrobials, at 1.10 per person per year, compared to 0.88 antimicrobials used per person per year in patients aged 0–64 years [50]. Antibiotics induce gut microbiome disturbances, persistent through constant presence in the food supply [51] or by introducing new and potentially stable changes with each cycle of antibiotic administration [52, 53]. Amidst these microbiota disturbances, the prevalence

of infection by opportunistic pathogens, including *C. difficile*, are dramatically overrepresented in elderly populations [13]. Finally, we evaluated if colonic organoids [54] reproduced the *in vivo* response to GOS. Our findings add further evidence to previous limited studies on age-associated dysbiosis and intestinal physiology, providing valuable insights into how dietary GOS impact the microbiome composition and functionality, intestinal barrier function, and biomarkers of inflammation in an animal model of aging.

Results

Analysis of the gut microbiome from the first group of old and young C57BL/6J SPF mice fed a control diet was done by 16S rRNA amplicon sequencing of stool samples. Young animals had a significantly higher diversity (Figure 1a) and a distinct composition (Figure 1b) compared to old animals [17]. While *Bacteroidetes*, followed by *Firmicutes* and *Proteobacteria* dominated both young and old mouse gut microbiome; old mice had a significantly (FDR corrected P = 0.01) higher abundance of *Verrucomicrobia* (10% in old versus 1.9% in young) and Unassigned bacteria (3.8% in old and 0.001% in young animals).

Assignment of bacterial taxa at the genus level to saccharolytic (SAC), non-saccharolytic (NON_SAC) or undetermined metabolism [71] showed specific differences between the old and the young cohorts. Old animals had a significant reduction in the overall abundance of saccharolytic bacteria (Mann-Whitney P<0.01) and an over-abundance of non-saccharolytic organisms (P<0.05) (Figure 1c). Old animals had a significantly (FDR corrected P =0.05) increased relative abundance of the *Akkermansia* and reduced *Bilophila* and *Mucispirillum* in the NON_SAC category. Within the SAC category, old animals had a significantly decreased relative abundance of *Bacteroides, Parabacteroides, Sutterella, Prevotella, Dehalobacterium, Ruminococcus, Christensenella, Desulfovibrio,* and *Allobaculum*. Conversely, abundance of *Anaerotruncus, Coprobacillus, Enterococcus, Anaerostipes, Lactococcus, Turicibacter, Bifidobacterium* and *Propionibacterium* were increased in this group (Figure 1d).

Impact of GOS and antibiotics on the gut microbiome

A second cohort of twenty-four young and old C57BL/6J female mice (N = 48) were fed the control diet for two weeks and then switched to the experimental diet containing prebiotics (Figure 2a). Analysis of 16S rRNA amplicon sequencing data performed on longitudinal timepoints 1 (T1, day 20, after normalization period), 2 (T2, day 35), 3 (T3, day 38), 4 (T4, day 42), and 5 (T5, day 50) assigned 190 distinct bacterial taxa at the species level. We observed a transient decrease in phylogenetic diversity in old and young animals receiving the prebiotics diet at T2, day 35 (ANOVA with pairwise comparisons $P<0.05$) (Figure 2b). Diversity recovered in young and old animals in the GOS groups at T3. However, the GOS groups had lower diversity after treatment with clindamycin (T4 and T5) compared to the control groups in old and young animals.

Analysis of saccharolytic and non-saccharolytic bacteria (Figure 2c) showed that GOS increased the relative abundance of saccharolytic and non-saccharolytic bacteria, driven by *Bacteroides* and *Akkermansia*, respectively (Figure S1), reducing the abundance of bacteria of undetermined metabolism at T2. Although the bifidogenic effect of GOS has been previously reported [41, 45, 47, 94], we did not observe a consistently significant increase in the abundance of bifidobacteria in these cohorts of old or young animals fed GOS diet. To investigate whether compositional differences were translated into potential functional discrepancies, we conducted Whole Genome Shotgun (WGS) of a subset of samples from control and GOS groups. WGS sequencing of stool samples showed a reduced proportion of bacterial EC:3.2.1. O-Glycosyl hydrolases in old mice, with increased representation of the enzymes in all mice fed the prebiotic (Figure 2d). Specifically, β-galactosidases (EC:3.2.1.23), which catalyze the hydrolysis of terminal, non-reducing beta-D-galactoside residues, and β-glucosidases (EC:3.2.1.21), which catalyze the hydrolysis of terminal, reducing beta-D-glucoside residues, and are hence essential for initial catabolism of GOS by primary degraders, were at a lower representation in old mice compared to young animals. GOS administration

resulted in increased the abundance of both β-galactosidases and β-glucosidases in young and old animals. GOS are broken down by bacterial enzymes, producing short-chain fatty acids including lactate and acetate [95]. In the healthy adult gut, secondary degraders including *Faecalibacterium* [96] and *Roseburia* [97] utilize these primary fermentation products to generate butyrate, which directly benefits host physiology [98-100].

In accordance with the clustering observed in the beta diversity analysis, administration of the antibiotic cocktail in water resulted in a temporary reversal of the observed results at T2. In contrast, the subsequent clindamycin IP injection resulted in a marked increase of saccharolytic bacteria and a reduction of bacteria of undetermined metabolism. Analysis at the genus level identified 48 taxa significantly changed from T4 to T5 upon clindamycin injection in at least one of the groups in our analysis (Old_control, Old_GOS, Young_control, Young_GOS) (Supplementary Text and Supplementary Figure 2). Interestingly, while the antibiotic decreased abundance of *Bifidobacterium* and *Lactobacillus* in young and old mice in both diets, clindamycin increased the relative abundance of non-saccharolytic bacteria in animals (young and old) receiving the control diet.

Although no differences in alpha diversity were observed between young and old animals after the 2-week normalization period, Principal Coordinate Analysis (PCoA) plots showed significant differences in microbiome composition between old and young mice, as well as between old and young animals fed either GOS or the control diet (ANOSIM R=0.45, P=0.001, PERMANOVA pseudo-F=3.8, P=0.001) at day 20 (T1) (Figure 3). We observed 3 clusters (numbered counter clockwise in Figure 3a), which persisted over time until T5 where a new cluster was formed. Old animals at T1 grouped in one separate cluster (Cluster 2) while young animals at T1 were included in Cluster 1, together with mice fed control diet at T2. Both old and young animals fed GOS diet were included in newly formed cluster (Cluster 3) at T2 (Figure 3a). Administration of the antibiotic cocktail in drinking water resulted in young and old animals “returning” to their original clusters at T1 suggesting that the antibiotics impacted the

newly blooming bacteria enhanced by the prebiotics (Figure 3b). However, the clusters observed at T2 were also observed at T4 suggesting recovery of the communities assembled in the GOS fed groups. Finally, after animals received an IP injection of clindamycin, community changes were observed in T5. Cluster 2, composed of old animals fed control or GOS diets, was replaced by two new groups: cluster 4, which included young and old animals fed GOS that received the antibiotic, and cluster 5 including samples from young and old animals fed the control diet that also received the antibiotic (Figure 3d). These results indicate a clear influence of diet on the response of the microbial community to clindamycin.

GOS impact on intestinal permeability, biomarkers of inflammation and mucin production

Assessment of gut barrier function showed significantly increased intestinal permeability in old compared to young mice, with decreased values in old animals fed GOS (Figure 4a-i). We did not detect a significant increase in permeability in antibiotic-treated young or old animals, probably because mice were allowed to recover for 7 days before euthanasia. Colon tissue staining revealed that old mice had less mucus than young mice (Figure 4a-iii) [18, 19]. GOS diets increased the mucus abundance and thickness in the lumen of old mice (Figure 4a), but a less pronounced effect was observed in young animals.

Epithelial surface integrity is maintained in part by genes in the trefoil factor (TFF) family including TFF3 [101]. TFF3 binds to the cysteine-rich amino terminal von Willebrand factor (vWF) of MUC2 enhancing protection of the gastrointestinal mucosa against injury through interactions with mucins [102]. The resistin-like molecule (RELM) family of proteins facilitate the formation of unique disulfide-dependent multimeric assembly units. RELMb is predominantly expressed by goblet cells and epithelial cells in the colon and is involved in the maintenance of colonic epithelial barrier function by up regulating *MUC2* [103]. Expression of *MUC2* was increased with GOS, while *RELMb* and *TFF3* showed non-significant increases (Figure 4a-ii).

Increased levels of circulating cytokines (plasma and serum) associated with aging have been reported in humans and mice [28, 104, 105]. A three-way ANOVA showed that the most

important factor in modulating levels of serum cytokines was antibiotic administration. The antibiotics groups had higher IL-17 and IL-6 levels in both control and GOS diets, higher IP-10 and eotaxin in control and lower IP-10 and eotaxin in GOS diets. Levels of IL-6 were higher in the GOS diet, regardless of age. Finally, young animals had higher levels of IL-13, regardless of diet. Although levels of serum tumor necrosis factor (TNF) α did not show significant differences between groups, we detected significantly increased gene expression of TNF α in old mice and prebiotics decreased expression of the cytokine (Figure 4b). Conversely, no significant differences in gene expression were detected for IL-6 by age nor by diet (not shown).

Colon mucosa transcriptome profiling showed significant differences in response to GOS diets between young and old mice

Covariate analysis of transcriptomics data from colon tissue of 6 versus 60-week-old mice fed the control or GOS diets showed clear patterns of gene expression (Figure 5, Supplementary Table 1). Old animals fed GOS had an increased representation of genes involved in the production of molecular mediators of immune response (GO:0002440) compared to old animals fed the control diet. Functions included immunoglobulin production, positive regulation of T-helper 1 cell cytokine production and positive regulation of immunoglobulin biosynthetic processes. Conversely, old animals fed GOS had a lower expression of genes in the collagen-containing extracellular matrix (GO:0062023), specifically a disintegrin-like and metallopeptidase (reprolysin type) with thrombospondin type 1 motif, collagen, type VI, alpha 1, fibronectin 1, and insulin-like growth factor binding protein 6 (Figure 5a).

The majority of genes (92 genes) over expressed in young compared to old animals fed the prebiotics diet were functionally associated with binding (GO:0005488), specifically protein binding (GO:0005515, 64 genes), ion binding (GO:0043167, 53 genes), and protein-containing complex binding (GO:0044877, 20 genes) (Figure 5b). In old animals fed GOS, genes involved in small molecule metabolic processes (GO:0044281) and specifically the respirasome

(GO:0070469) were over expressed compared to young animals on the same diet (Figure 5c). In young mice, GOS also stimulated the expression of the galectin gene *Lgals1*, a β-galactosyl-binding lectin that bridges molecules by their sugar moieties, forming a signaling and adhesion network [106]. Accordingly, further analysis of gene expression differences by mapping onto the Kyoto Encyclopedia of Genes and Genomes (KEGG) metabolic maps (www.genome.jp/kegg/) showed higher expression levels of genes in focal adhesion, PI3K-Akt and ECM-receptor interaction pathways [107] in young compared to old animals. The lowest expressed gene in both old and young animals fed GOS was *Trpv6* (transient receptor potential cation channel, subfamily V, member 6), a highly selective calcium channel that acts via calcium absorption in the intestine and kidney [108]. This gene was over expressed in young compared to old animals both on the GOS and control diets.

Responders *versus* non-responders to GOS diets

It has been previously reported that, when fed GOS, a proportion of individuals will not mount a bifidogenic response [41, 45, 47], i.e., they will not display an appreciable increase in the relative abundance of bifidobacteria. In this study, we injected stools from responder and non-responder mice (Figure 6) into colon organoids from the same genetic background to better understand the magnitude of the microbiome role in the bifidogenic effect of GOS diets. Stools from individual mice were processed, mixed with either GOS, lactose or PBS (control), and injected into organoids derived from colon as previously described [109]. Organoids were collected immediately, 24 and 72 hours after injection for 16S rRNA amplicon sequencing. Quantitative PCR showed that the response and non-response phenotypes were reproduced in the organoids injected with stools from young mice; however, all organoids injected with stools from old mice showed an increased relative abundance of *Bifidobacterium* (Figure 6a). In general, the abundance of bifidobacteria in organoids was one order of magnitude higher than *Bifidobacterium* abundance *in vivo*.

Shannon diversity index and species richness values showed a rapid reduction soon after injection (Figure 6b), with no significant differences at any time (except stool baseline) between treatments (GOS, lactose, control) or between young and old samples, in contrast with the GOS diversity decrease observed *in vivo*. Principal Coordinate Analysis (PCoA) of samples showed compositional significant differences between groups by age (Bonferroni-corrected nonparametric *P*-value = 0.01) and time (*P* = 0.02), while overall differences in microbiome composition between lactose and GOS-treated organoids approached significance (*P* = 0.06).

At the compositional level we observed clear differences between the original stool samples processed for injection, the microbiome of organoids injected with young *versus* old samples, and between the different treatments (control, GOS and lactose) (Supplementary Figures 3 and 4, and Supplementary Text). Our analysis allowed us to identify bacterial groups especially sensitive to manipulation, which could be drastically eliminated from the stool sample upon processing for injection into the organoids, creating the niche for expansion of groups originally in very low numbers.

Discussion

Our study confirmed previous reports indicating increased intestinal permeability (a "leaky gut") during aging [19, 28]. Likewise, old mice had a distinct microbiome characterized by lower diversity, increased ratios of non-saccharolytic *versus* saccharolytic bacteria and, correspondingly, lower abundance of O-Glycosyl hydrolases (EC:3.2.1.). Based on numerous studies detailing the beneficial effects of prebiotic GOS, which include modulation of the gut microbiome with specific increases in beneficial bacteria [45, 47], stimulation of tight junctions and enhancement of the intestinal barrier function through modulation of goblet cells [38], reduction of inflammatory markers release in cell culture models [39], support of intestinal development and mucosal immune responses [40], and reduction in adherence of enteropathogenic *Escherichia coli* to tissue culture cells [110], we designed a short-term feeding

trial to determine the effects of GOS on the aging gut microbiome and gut homeostasis. Our study also aimed to assess the transient effects of GOS on gut responses to antibiotic administration.

Consistent with previously reported data [17], old mice had a distinctive gut microbiome, with lower phylogenetic diversity, increased representation of *Rikenella,* and a lower representation of di-, oligo-, and polysaccharide utilization genes. Human elderly populations have a reported reduction in the abundance of *Bifidobacterium*, *Faecalibacterium prausnitzii* and *Clostridium* XIVa [2-4]. In contrast with these reports, our cohort of old mice had an over representation of bifidobacteria and similar proportions of *Faecalibacterium* compared to young mice after the normalization period at day 20. Also in contrast with a previous report [17], old animals had a significantly higher abundance of *Akkermansia*. *A. muciniphila* has been shown to reduce inflammation [111] and improve intestinal barrier integrity [112] suggesting that controlled mucolytic activity likely results in benefits to host physiology. However, uncontrolled degradation of mucins by proteolytic bacteria can increase inflammation, damage the barrier integrity, and increase susceptibility to pathogen infection [28, 113]. Finally, old mice had a lower representation of *Bacteroides*. Although highly variable, the abundance of *Bacteroides* in aging human individuals is also lower than in the adult population [114]. GOS had a clear impact on composition of the gut microbiome, increasing abundance of both non-saccharolytic (*A. muciniphila* in particular) and saccharolytic bacteria (species of the genus *Bacteroides,* unknown species of the order *Bacteroidales*, and species of *Lactobacillus*). It has been previously reported that dietary GOS increased the abundance of bifidobacteria in human adults [41, 47] and older adults [94]. We also showed that GOS induced a variable bifidogenic response in 8-12 week-old mice [45]. In this study, we did not observe an overall significant increase in the abundance of bifidobacteria in old or young animals fed the GOS diet. However, old mice did have a reduced proportion of bacterial O-Glycosyl hydrolases, suggesting a reduction in metabolic potential of the microbiota. When fed GOS diets, both old and young animals showed

an increased abundance of β-galactosidases and β-glucosidases genes. Reduced expression of intestinal saccharolytic enzymes in the aging gut has been reported (although data is not conclusive) [115, 116] and may have important nutritional implications for the digestion of dietary carbohydrates by elderly individuals. Finally, administration of the GOS diet reduced bacterial diversity significantly in young and old mice. This is in accordance with studies of GOS-supplemented infant formula [117] and in contrast with previous studies on human adults [47, 118] and young or adult BALB/c mice that showed no effect of GOS on bacterial diversity [119, 120].

Clindamycin, depending on the organism, infection site and concentration can act as a bacteriostatic or bactericidal antibiotic. This antibiotic prevents the formation of peptide bonds effectively inhibiting protein synthesis by binding to the 50S ribosomal subunit. Clindamycin palmitate is hydrolyzed in the gastrointestinal tract and then distributed across the body [121]. This antibiotic has been associated to a high incidence of antibiotic-associated diarrhea [122]. In our study, the antibiotic caused an expected decreased abundance of *Bifidobacterium* and *Lactobacillus* in young and old mice on both diets. This is in agreement with a previous *in vitro* report that showed that, in contrast with the antibiotics tetracycline and ciprofloxacin, GOS feeding after clindamycin administration did not result in increased abundance or recovery of bifidobacteria populations [123]. Interestingly, the abundance of non-saccharolytic (*Akkermansia*) bacteria was actually increased in young and old animals that received clindamycin but only in animals receiving the control diet. Our results warrant further research on the effect of diet on the microbiome response to clindamycin in the aging gut.

Transcriptomics analysis of colon at the end of the experiment indicated that GOS impacted intestinal expression differently in young compared to old mice. Young animals had a significant enrichment in binding-related genes (GO:0005488). GOS also stimulated the expression of the galectin gene *Lgals1*, a β-galactosyl-binding lectin that bridge molecules by their sugar moieties, forming a signaling and adhesion network [106]. Glycosylation in intestinal

epithelial goblet cells is essential for the protection of the epithelium by the mucus, which is largely composed of highly glycosylated mucins. A previous *in vitro* study showed that butyrate stimulated expression of *Lgals1* in the HT29-C1.16E, a clonal derivative of the HT29 human colonic cells [100]. As extensively reported, GOS fermentation by intestinal microorganisms results, via cross-feeding events, in the generation of short chain fatty acids (SCFAs) [95], which directly influence host intestinal physiology [98, 124]. SCFAs including butyrate are utilized by intestinal epithelial cells as an energy source, promoting host epithelial metabolism [125], and can also be used as signaling molecules, influencing host inflammation [98, 126], stem cell proliferation [127], and barrier integrity [99, 126].

Further analysis showed higher expression levels of genes in focal adhesion, PI3K-Akt and ECM-receptor interaction pathways [107]. Cell-matrix adhesions play essential roles in cell motility, cell proliferation, cell differentiation, regulation of gene expression and cell survival. At the cell-extracellular matrix contact points, specialized structures (focal adhesions), collections of actin filaments anchored to transmembrane receptors of the integrin family through a multi-molecular complex of junctional plaque proteins, act as structural links between membrane receptors and the actin cytoskeleton, or as signaling molecules, including different protein kinases and phosphatases, their substrates, and various adapter proteins [128, 129]. Old animals fed the GOS diet had increased expression of genes involved in small molecule metabolic processes (GO:0044281) and specifically the respirasome (GO:0070469). Although the role of this respiratory enzymes organized into super complexes in the intestine has not been defined, it can be hypothesized they could reduce oxidative damage increasing metabolism efficiency [130, 131].

Microbiome research using colonic organoids as an *in vitro* platform is at its infancy [54, 132]. In this study, we took advantage of this platform to determine if the response/non-response to prebiotics [41, 45, 47] could be replicated *in vitro*. Injections of stools showed that the response and non-response phenotypes was reproduced in the organoids injected with

stools from young mice. However, all organoids injected with stools from old mice showed an increased relative abundance of *Bifidobacterium*. Stool-injected organoids showed a rapid decrease in bacterial diversity after injection and showed compositional significant differences between groups by age, time and treatment. The analysis of microbiome composition over time allowed us to identify bacterial groups especially sensitive to manipulation that were radically eliminated from the stool sample upon processing for injection into the organoids, creating the niche for expansion of groups originally in very low numbers in the stool samples.

The most remarkable effect of prebiotics in the old animals was the reduction on intestinal permeability via increased mucus biosynthesis. Defects in the intestinal barrier associated with aging have been previously reported [133, 134]. A relevant study by Thevaranjan et al [28] reported that intestinal permeability increased with age due to age-associated microbial dysbiosis. In their study, increased permeability led to increased systemic inflammation with high levels of serum IL-6. In contrast, although our cohort of old animals had significantly higher intestinal permeability than young mice, there were not significant differences in serum IL-6 or serum TNFα between old and young mice. However, we observed increased TNFα expression in old animals, which was ameliorated by GOS. Our study suggests that GOS modulation of intestinal homeostasis occurs through direct GOS-host interactions (induction of *MUC2* and increased mucus production) as well as interactions mediated by the gut microbiota (increased saccharolytic function).

Conclusions

By looking at a conjunction of host and microbiota metagenomics/transcriptomics and physiological assays, we are able to conclude that the beneficial characteristics of dietary prebiotic GOS occur through multiple different pathways, and that these benefits include, but extend beyond modulation of the gut microbiota. Specifically, GOS induces expression of the

Muc2 gene in mice, increasing production of mucus and subsequently providing a thinker intestinal mucin layer providing reduced intestinal permeability. Similarly, consumption of GOS modulates systemic inflammatory signaling, providing new insights into how the gut microbiota may play critical roles in systems beyond the gastrointestinal tract. A major novel finding in regard to microbiota modulation by GOS was that the abundance of *Akkermansia muciniphila*, a mucin-degrading microorganism emerging as a potential probiotic, was increased with GOS-feeding. Host gene expression profiles indicate that there is an age-specific response to prebiotic feeding, suggesting that differences in physiology between old and young animals may influence how these animals respond to dietary treatments. Finally, our findings suggest that response to dietary GOS is not only dependent on the gut microbiota, but also varies based on host genetics. Together these findings lay the groundwork for new studies focusing on the impacts of prebiotics on host metabolism and systemic modulation of inflammation by the gut microbiota.

Methods

Animal housing, treatment, and sample collection

For initial microbiota studies, 24 mice, ages 4-8 weeks (N=12) and 64-84 (N=12) weeks old were used to determine differences in the microbiome of old versus young animals. Mice of the C57BL/6J background were acquired from Jackson Laboratory (Bar Harbor, ME) and kept under specific pathogen free (SPF) conditions. Animals were co-housed and fed a control diet (Growth Purified Diet AIN-93G ENVIGO TD.94045) for 14 days to promote a homogenous gut microbiota (Table S1). Stool samples were collected weekly for 3 weeks.

For the second animal experiment, 48 female mice (24 6-week-old and 24 60-week-old) received a control diet (D17121301; Research Diets INC.) for a two-week co-housed (6/cage) normalization period. Animals were subsequently paired off (1 old/1 young) from different normalization cages and separated into groups fed control or GOS diets, using an optimized

GOS diet (D17121302; Research Diets INC.) replacing 71.8g of cellulose with 71.8g of pure GOS per kilogram. Pure prebiotics were generated by heterologous expression of the beta-hexosyl transferase from *Sporobolomyces singularis* in *Pichia pastoris* as previously described [45, 49] After two weeks, half of the animals in each group (6 young and 6 old from each diet) were administered an antibiotic cocktail in their drinking water for 3 days according to the protocol described by Chen et al [55]. The cocktail contained: kanamycin (40mg/kg), gentamycin (3.5mg/kg), colistin (4.2mg/kg), metronidazole (21.5mg/kg), and vancomycin (4.5mg/kg). The concentrations of antibiotics in water were calculated based on the average weight and expected water consumption of mice. After three days, the water was replaced with antibiotic-free water and the animals were allowed two days to recover prior to receiving an intraperitoneal injection of clindamycin (10µg/g body weight). Animals remained on their respective diets and were sacrificed following a one-week recovery period. For both experiments, fresh stool samples were collected and stored at -80°C. Intestinal tissues and contents were collected at termination (Figure 2a)

Mouse Intestinal Permeability Assay

Mice were administered 100mg fluorescein isothiocyanate (FITC) dextran/100g body weight via oral gavage 4 hours prior to sacrifice. Immediately following euthanasia, blood was harvested via cardiac puncture and serum was subsequently separated via centrifugation. Serum from each animal was assayed for the presence and quantity of FITC signal with a TECAN Infinite M200 plate reader, using an excitation wavelength of 485 nm and emission wavelength of 528 nm. A standard curve of FITC dextran was used to quantify the signal in each serum sample.

Mucin Staining and Tissue Imaging

Sections of mouse distal colon were harvested, embedded in optimal cutting temperature (OCT) compounding agent and flash-frozen in a dry ice filled ethanol bath without

fixation. Blocks were stored at -80C until cut at -20C on a cryostat and frozen sections were mounted onto slides. Sections were immediately subject to paraformaldehyde vapor fixation (4% PFA, 60C) for 8 hours prior to PAS staining and subsequent imaging on Nikon 2000-E inverted widefield microscope.

Organoid Cultivation and Colonization

Organoids were derived from mouse colon crypts and grown in 96-well plates embedded in matrigel overlaid with complex DMEM-F12 growth media containing 1µg/ml Pen Strep [56, 57]. Organoids were incubated at 37ºC under 5% CO_2 and ambient oxygen and were passaged into new plates every 10-14 days. Organoids used for injection were grown 4 days post-passage and were uniform in size and shape. Homogenized stool samples were filtered through 5µM syringe filters (Millipore) and loaded into microinjection needles for organoid inoculation as previously described [58]. Loaded needles were attached to injection apparatus, and organoids were injected with ~400pL of stool suspension. Injected organoids were then incubated at 37°C under 5% CO_2 and ambient oxygen with supplemental antibiotics. Organoids were harvested at 0h, 24h, and 72h post-injection.

Nucleic Acid Isolation

DNA from fecal samples and microbiota-colonized organoids were extracted using the Qiagen DNeasy stool DNA isolation kit (Qiagen, Valencia, CA) with an additional bead-beating step aimed to ensure uniform lysis of bacterial spores. Samples were loaded into tubes containing 10mg of sterile, acid washed, 1um glass beads and homogenized for 5 minutes at 15Hz in Qiagen TissueLyser II (Qiagen, Valencia, CA). DNA was subsequently used for 16S rRNA amplicon sequencing and whole genome shotgun sequencing. RNA isolation from tissues was performed using Qiagen RNeasy kit (Qiagen, Valencia, CA) following manufacturer's instructions for subsequent use in RTqPCR and mRNA sequencing.

High-throughput quantitative PCR detection of *Bifidobacterium*

The Access array AA 24.192 (Fluidigm Corporation, San Francisco, CA) was used in the UNC Advanced Analytics Core. Primers for amplification of the 16S rRNA gene and GroEL have been validated in previous studies [59-62]. The taxonomic groups targeted in the *Bifidobacterium* array include: domain *Bacteria*, phylum *Actinobacteria*, genus *Bifidobacterium* and *Bifidobacterium* species. Pre-amplification (specific target amplification, STA) assays and microfluidic qPCR were be performed on a BioMark HD reader as described [45]. Raw data were normalized using the Livak method[63]. Cq values for each sample were normalized against their respective Cq value obtained from universal primers using the equation: Ratio (reference/target) = $2^{-Ct\ (ref)-Ct\ (target)}$.

16S rRNA Amplicon Sequencing

Total DNA was subject to amplification of the V4 region of the 16S rRNA gene using primers (515F-806R) with Illumina adaptors. Amplicons were barcoded using Illumina dual-index barcodes (Index 1(i7) and Index 2(i5)), purified using Agencourt® AMPure® XP Reagent (Beckman Coulter, Brea, CA) and quantified with Quant-iT™ PicoGreen® dsDNA Reagent (Molecular Probes, Thermo Fisher Scientific, Waltham, MA). Libraries were pooled in equimolar amounts and sequenced on MiSeq (Illumina, San Diego, CA).

Data analysis: 16S rRNA amplicon sequencing data analysis was carried out using the QIIME pipeline [64] as described [45, 65-67]. Briefly, sequences were grouped into Operational Taxonomic Units (OTUs) using UCLUST [68]. OTU sequences were aligned and phylogenetic trees were built [69]. OTU tables were used to perform alpha and beta diversity calculations, measurements that were used with sample metadata to create graphic visualizations for scientific interpretation. A combination of Unifrac significance and Principal Coordinate Analysis, (PCoA) using Fast Unifrac [70] was done to compare samples based on age, time, genotype, and prebiotic feeding.

Assignment of saccharolytic (SAC) and non-saccharolytic (NON_SAC) to bacterial taxa

We used the reference study by Vieira-Silva et al. [71], which mined 532 publicly available gut reference genomes and assigned them to four different groups (proteolytic, saccharolytic, lipolytic and generalist bacteria) using metagenome analytical methods, and the study by Magnusdottir et al. [72] on the metabolic reconstruction network AGORA. In the case that the genus was not categorized in the mentioned studies we referred to the Bergey's Manual of Systematic Bacteriology [73] and previously published reports when the genus was not found in either source [74-85]. We included saccharolytic and generalist bacteria in the SAC group, as well as chemolithoheterotrophic bacteria capable of using either carbohydrates or the metabolites derived from carbohydrate sources (for example, *Dehalobacter, Geobacillus*). Likewise, the NON_SAC category included proteolytic and lipolytic bacteria.

Whole Genome Shotgun (WGS) Sequencing

1ng of intact genomic DNA was processed using the Nextera XT DNA Sample Preparation Kit (Illumina, San Diego, CA). In this process target DNA was simultaneously fragmented and tagged by the Nextera Enzyme Mix containing transposome, which fragments the input DNA and adds bridge PCR (bPCR)-compatible adaptors required for binding and clustering on the flow cell. Next, fragmented DNA was amplified via a limited-cycle PCR program adding index 1(i7) and index 2(i5) (Illumina) in unique combination for each sample, as well as primer sequences required for cluster formation. Libraries were purified using Agencourt® AMPure® XP Reagent (Beckman Coulter, Brea, CA) and quantified with Quant-iT™ PicoGreen® dsDNA Reagent (Molecular Probes, Thermo Fisher Scientific, Waltham, MA). All libraries were pooled in equimolar amounts and heat denatured before loading on Illumina HiSeq2000 Rapid.

Data analysis: Sequencing output from the Illumina platform was converted to fastq format and demultiplexed using Illumina Bcl2Fastq 2.18.0.12. Quality control of the demultiplexed sequencing reads were verified by FastQC. The resulting paired-end reads were aligned with

Bowtie2 [86] against the host reference and all aligning reads will be eliminated. Paired-end reads were joined with vsearch 1.10.2. The resulting single-end reads were again aligned against the reference with Bowtie2 retaining all reads that did not align. Estimates of taxonomic composition, gene family, path abundance, and path coverage were produced from the remaining reads using HUMAnN2 [87].

Reverse Transcription qPCR

30µg of total RNA was subject to reverse transcription using iScript Advanced cDNA synthesis kit (Bio-Rad, Hercules, CA). Specific target amplification was performed on cDNA using the following primers: GapDH (Fwd: 5'-TGCACCACCACCAACTGCTTAG-3', Rev: 5'-GGATGCAGGGATGATGTTC-3') [88], Muc2 (Fwd: 5'-GCTGACGAGTGGTTGGTGAATG-3', Rev: 5'-GATGAGGTGGCAGACAGGAGAC-3') [89], RELMβ (Fwd: 5'-CCATTTCCTGAGCTTTCTGG-3', Rev: 5'-AGCACATCCAGTGACAACCA-3') [90], and TFF3 (Fwd: 5'-CAGATTACGTTGGCCTGTCTCC-3', Rev: 5'-ATGCTTGCTACCCTTGGACCAC-3') [90]. qPCR reactions were performed using Power SYBR Green Master Mix on the QuantStudio Q6 instrument (Thermo Fisher Scientific, Waltham, MA).

Mouse mRNA sequencing

Total RNA isolated from mouse colon was processed using the NuGEN Universal Plus mRNA-Seq kit (NuGEN Technologies, Inc., San Carlos, CA) for whole transcriptome sequencing as directed by the manufacturer. Briefly, total RNA was subject to poly(A) selection, fragmentation, first strand synthesis, second strand synthesis, end repair, adaptor ligation, strand selection, and finally library amplification. Indexed cDNA libraries quantified via Quant-iT^{TM} PicoGreen® dsDNA reagent (Thermo Fisher Scientific, Waltham, MA), were pooled at equimolar concentrations and sequenced on Illumina HiSeq4000 platform.

Data analysis: Demultiplexed paired-end reads from mRNA sequencing experiments were

aligned with STAR [91] against the mouse Mm9 reference. Salmon [92] was applied to the resulting alignment to estimate quantity of transcript expression. Significance of differential expression was measured with DESeq2 [93].

Cytokine analysis

In order to study the impact of dietary GOS supplementation on inflammatory biomarkers, serum from mice was subject to Milliplex cytokine/chemokine assay MCYTOMAG-70K (Millipore, Sigma, Burlington, MA) for detection and quantification of TNFα, IP-10, IL-17, IL-13, IL-10, IL-6, IL-4, IL-1α, Eotaxin, IL-12, and IL-7. Assay was run at the UNC Advanced Analytics Core on DropArray^{TM}96 Plate system (Curiox Biosystems, San Carlos, CA) as recommended by the manufacturer.

Statistical analyses

Pairwise comparisons were tested for statistical significance using ANOVA with ad-hoc Tukey test and P-values were reported accordingly. For comparison of sequencing data, Bonferroni correction was applied to the statistical analysis of samples to take into consideration multiple comparisons. Cutoff for statistical significance was set to $p<0.01$ for microbiota analyses, gene expression, and intestinal permeability assays. For cytokine analysis, due to low numbers of samples, $p<0.1$ was the cutoff set for significance.

Declarations

Ethics approval: All live animal studies were approved by the Institutional Animal Care and Use Committee (IACUC) of the University of North Carolina at Chapel Hill (Approved protocol numbers: 10-197, 16-080.0).

Consent for publication: Not applicable

Availability of data and materials: All sequencing data has been submitted to NCBI repository and can be accessed via the following accession numbers: Mouse Microbiota 16S rRNA Amplicon Sequencing PRJNA605460, Whole Genome Shotgun Sequencing: PRJNA605640,

Mouse mRNA Sequencing: PRJNA605019, Organoid 16S rRNA Amplicon Sequencing: PRJNA606062.

Competing interests: The authors declare that they have no competing interests.

Funding: This work was supported by the NC State University Chancellor's Innovation Fund (1108) 2018-2092). The UNC Microbiome Core is supported in part by the NIH grant P30 DK034987. R.T. is supported by NIH AI107029. S.F. received a postdoctoral fellowship from the Mexican Council on Science and Technology (CONACyT), grant number 205127.

Authors' contributions: Conceptualization, J. A., and M. A. A.-P.; Methodology, J.A., M. A. A.-P., S. M., S. F.; Formal Analysis, J. A., M. A. A.-P. and J. R.; Investigation, J. A. and S. F.; Resources, E. M., S. D., E. B., S. M., R. T., J. M. B., and M. A. A.-P.; Data Curation, J. A., S. F., and J. R.; Writing – Original Draft, J. A., and M. A. A.-P.; Writing – Review & Editing, J. A., M. A. A.-P.; R. T., S. F., J. M. B., and J. R.; Visualization, J. A., and M. A. A.-P.; Supervision, M. A. A.-P.; Project Administration, M. A. A.-P.; Funding Acquisition, M. A. A.-P., J. M. B., R. T., and S. F.

Acknowledgements:

Thank you to Dr. Natasha Snyder's lab, especially Rachel Battaglia for assistance with mouse tissue harvest.

References

1. Mitsuoka, T., *Intestinal flora and aging.* Nutr Rev, 1992. **50**(12): p. 438-46.
2. Biagi, E., et al., *Through ageing, and beyond: gut microbiota and inflammatory status in seniors and centenarians.* PLoS One, 2010. **5**(5): p. e10667.
3. Mueller, S., et al., *Differences in fecal microbiota in different European study populations in relation to age, gender, and country: a cross-sectional study.* Appl Environ Microbiol, 2006. **72**(2): p. 1027-33.
4. Hayashi, H., et al., *Molecular analysis of fecal microbiota in elderly individuals using 16S rDNA library and T-RFLP.* Microbiol Immunol, 2003. **47**(8): p. 557-70.
5. Mariat, D., et al., *The Firmicutes/Bacteroidetes ratio of the human microbiota changes with age.* BMC Microbiol, 2009. **9**: p. 123.
6. Rajilic-Stojanovic, M., et al., *Development and application of the human intestinal tract chip, a phylogenetic microarray: analysis of universally conserved phylotypes in the abundant microbiota of young and elderly adults.* Environ Microbiol, 2009. **11**(7): p. 1736-51.

7. Woodmansey, E.J., et al., *Comparison of compositions and metabolic activities of fecal microbiotas in young adults and in antibiotic-treated and non-antibiotic-treated elderly subjects.* Appl Environ Microbiol, 2004. **70**(10): p. 6113-22.
8. Bartosch, S., et al., *Characterization of bacterial communities in feces from healthy elderly volunteers and hospitalized elderly patients by using real-time PCR and effects of antibiotic treatment on the fecal microbiota.* Appl Environ Microbiol, 2004. **70**(6): p. 3575-81.
9. van Tongeren, S.P., et al., *Fecal microbiota composition and frailty.* Appl Environ Microbiol, 2005. **71**(10): p. 6438-42.
10. Tiihonen, K., et al., *The effect of ageing with and without non-steroidal anti-inflammatory drugs on gastrointestinal microbiology and immunology.* Br J Nutr, 2008. **100**(1): p. 130-7.
11. Makivuokko, H., et al., *The effect of age and non-steroidal anti-inflammatory drugs on human intestinal microbiota composition.* Br J Nutr, 2010. **103**(2): p. 227-34.
12. Tiihonen, K., A.C. Ouwehand, and N. Rautonen, *Human intestinal microbiota and healthy ageing.* Ageing Res Rev, 2010. **9**(2): p. 107-16.
13. Shin, J.H., K.P. High, and C.A. Warren, *Older Is Not Wiser, Immunologically Speaking: Effect of Aging on Host Response to Clostridium difficile Infections.* J Gerontol A Biol Sci Med Sci, 2016. **71**(7): p. 916-22.
14. Drekonja, D., et al., *Fecal Microbiota Transplantation for Clostridium difficile Infection: A Systematic Review.* Ann Intern Med, 2015. **162**(9): p. 630-8.
15. Konturek, P.C., et al., *Emerging role of fecal microbiota therapy in the treatment of gastrointestinal and extra-gastrointestinal diseases.* J Physiol Pharmacol, 2015. **66**(4): p. 483-91.
16. Rampelli, S., et al., *Functional metagenomic profiling of intestinal microbiome in extreme ageing.* Aging (Albany NY), 2013. **5**(12): p. 902-12.
17. Langille, M.G., et al., *Microbial shifts in the aging mouse gut.* Microbiome, 2014. **2**(1): p. 50.
18. Elderman, M., et al., *The effect of age on the intestinal mucus thickness, microbiota composition and immunity in relation to sex in mice.* PLoS One, 2017. **12**(9): p. e0184274.
19. Sovran, B., et al., *Age-associated Impairment of the Mucus Barrier Function is Associated with Profound Changes in Microbiota and Immunity.* Sci Rep, 2019. **9**(1): p. 1437.
20. Kobayashi, A., et al., *The functional maturation of M cells is dramatically reduced in the Peyer's patches of aged mice.* Mucosal Immunol, 2013. **6**(5): p. 1027-37.
21. Arike, L., J. Holmen-Larsson, and G.C. Hansson, *Intestinal Muc2 mucin O-glycosylation is affected by microbiota and regulated by differential expression of glycosyltranferases.* Glycobiology, 2017. **27**(4): p. 318-328.
22. Arike, L. and G.C. Hansson, *The Densely O-Glycosylated MUC2 Mucin Protects the Intestine and Provides Food for the Commensal Bacteria.* J Mol Biol, 2016. **428**(16): p. 3221-3229.
23. Johansson, M.E., et al., *Normalization of Host Intestinal Mucus Layers Requires Long-Term Microbial Colonization.* Cell Host Microbe, 2015. **18**(5): p. 582-92.
24. van Beek, A.A., et al., *Supplementation with Lactobacillus plantarum WCFS1 Prevents Decline of Mucus Barrier in Colon of Accelerated Aging Ercc1(-/Δ7) Mice.* Front Immunol, 2016. **7**: p. 408.
25. van der Lugt, B., et al., *Akkermansia muciniphila ameliorates the age-related decline in colonic mucus thickness and attenuates immune activation in accelerated aging Ercc1 (-/Δ7) mice.* Immun Ageing, 2019. **16**: p. 6.

26. Karav, S., G. Casaburi, and S.A. Frese, *Reduced colonic mucin degradation in breastfed infants colonized by Bifidobacterium longum subsp. infantis EVC001.* FEBS Open Bio, 2018. **8**(10): p. 1649-1657.
27. Schroeder, B.O., et al., *Bifidobacteria or Fiber Protects against Diet-Induced Microbiota-Mediated Colonic Mucus Deterioration.* Cell Host Microbe, 2018. **23**(1): p. 27-40.e7.
28. Thevaranjan, N., et al., *Age-Associated Microbial Dysbiosis Promotes Intestinal Permeability, Systemic Inflammation, and Macrophage Dysfunction.* Cell Host Microbe, 2017. **21**(4): p. 455-466 e4.
29. Maijo, M., et al., *Nutrition, diet and immunosenescence.* Mech Ageing Dev, 2014. **136-137**: p. 116-28.
30. Vasto, S., et al., *Inflammatory networks in ageing, age-related diseases and longevity.* Mech Ageing Dev, 2007. **128**(1): p. 83-91.
31. Sarkar, D. and P.B. Fisher, *Molecular mechanisms of aging-associated inflammation.* Cancer Lett, 2006. **236**(1): p. 13-23.
32. Butto, L.F. and D. Haller, *Dysbiosis in intestinal inflammation: Cause or consequence.* Int J Med Microbiol, 2016. **306**(5): p. 302-309.
33. Carding, S., et al., *Dysbiosis of the gut microbiota in disease.* Microb Ecol Health Dis, 2015. **26**: p. 26191.
34. Buford, T.W., *(Dis)Trust your gut: the gut microbiome in age-related inflammation, health, and disease.* Microbiome, 2017. **5**(1): p. 80.
35. Azcarate-Peril, M.A., et al., *Analysis of the genome sequence of Lactobacillus gasseri ATCC 33323 reveals the molecular basis of an autochthonous intestinal organism.* Applied and Environmental Microbiology, 2008. **74**(15): p. 4610-25.
36. Vandenplas, Y., I. Zakharova, and Y. Dmitrieva, *Oligosaccharides in infant formula: more evidence to validate the role of prebiotics.* Br J Nutr, 2015. **113**(9): p. 1339-44.
37. Akkerman, R., M.M. Faas, and P. de Vos, *Non-digestible carbohydrates in infant formula as substitution for human milk oligosaccharide functions: Effects on microbiota and gut maturation.* Crit Rev Food Sci Nutr, 2019. **59**(9): p. 1486-1497.
38. Bhatia, S., et al., *Galacto-oligosaccharides may directly enhance intestinal barrier function through the modulation of goblet cells.* Mol Nutr Food Res, 2015. **59**(3): p. 566-73.
39. Akbari, P., et al., *Galacto-oligosaccharides Protect the Intestinal Barrier by Maintaining the Tight Junction Network and Modulating the Inflammatory Responses after a Challenge with the Mycotoxin Deoxynivalenol in Human Caco-2 Cell Monolayers and B6C3F1 Mice.* J Nutr, 2015. **145**(7): p. 1604-13.
40. Alizadeh, A., et al., *The piglet as a model for studying dietary components in infant diets: effects of galacto-oligosaccharides on intestinal functions.* Br J Nutr, 2016. **115**(4): p. 605-18.
41. Davis, L.M., et al., *Barcoded pyrosequencing reveals that consumption of galactooligosaccharides results in a highly specific bifidogenic response in humans.* PLoS One, 2011. **6**(9): p. e25200.
42. Scalabrin, D.M., et al., *New prebiotic blend of polydextrose and galacto-oligosaccharides has a bifidogenic effect in young infants.* Journal of pediatric gastroenterology and nutrition, 2012. **54**(3): p. 343-52.
43. Salvini, F., et al., *A specific prebiotic mixture added to starting infant formula has long-lasting bifidogenic effects.* The Journal of nutrition, 2011. **141**(7): p. 1335-9.
44. Rowland, I.R. and R. Tanaka, *The effects of transgalactosylated oligosaccharides on gut flora metabolism in rats associated with a human faecal microflora.* The Journal of applied bacteriology, 1993. **74**(6): p. 667-74.

45. Monteagudo-Mera, A., et al., *High purity galacto-oligosaccharides enhance specific Bifidobacterium species and their metabolic activity in the mouse gut microbiome.* Benef Microbes, 2016. **3**: p. 1-18.
46. Azcarate Peril, M.A., et al., *Microbiome alterations of lactose intolerant individuals in response to dietary intervention with galacto-oligosaccharides may help negate symptoms of lactose intolerance.* Gastroenterology, 2013. **144**(5): p. S-893.
47. Azcarate-Peril, M.A., et al., *Impact of short-chain galactooligosaccharides on the gut microbiome of lactose-intolerant individuals.* Proc Natl Acad Sci U S A, 2017. **114**(3): p. E367-E375.
48. Vulevic, J., et al., *Modulation of the fecal microflora profile and immune function by a novel trans-galactooligosaccharide mixture (B-GOS) in healthy elderly volunteers.* Am J Clin Nutr, 2008. **88**(5): p. 1438-46.
49. Dagher, S.F., M.A. Azcarate-Peril, and J.M. Bruno-Barcena, *Heterologous expression of a bioactive beta-hexosyltransferase, an enzyme producer of prebiotics, from Sporobolomyces singularis.* Appl Environ Microbiol, 2013. **79**(4): p. 1241-9.
50. Giarratano, A., S.E. Green, and D.P. Nicolau, *Review of antimicrobial use and considerations in the elderly population.* Clin Interv Aging, 2018. **13**: p. 657-667.
51. Van Boeckel, T.P., et al., *Global trends in antimicrobial use in food animals.* Proc Natl Acad Sci U S A, 2015. **112**(18): p. 5649-54.
52. Dethlefsen, L. and D.A. Relman, *Microbes and Health Sackler Colloquium: Incomplete recovery and individualized responses of the human distal gut microbiota to repeated antibiotic perturbation.* Proc Natl Acad Sci U S A.
53. Dethlefsen, L. and D.A. Relman, *Incomplete recovery and individualized responses of the human distal gut microbiota to repeated antibiotic perturbation.* Proc Natl Acad Sci U S A, 2011. **108 Suppl 1**: p. 4554-61.
54. Williamson, I.A., et al., *A High-Throughput Organoid Microinjection Platform to Study Gastrointestinal Microbiota and Luminal Physiology.* Cell Mol Gastroenterol Hepatol, 2018. **6**(3): p. 301-319.
55. Chen, X., et al., *A mouse model of Clostridium difficile-associated disease.* Gastroenterology, 2008. **135**(6): p. 1984-92.
56. Gracz, A.D., et al., *A high-throughput platform for stem cell niche co-cultures and downstream gene expression analysis.* Nat Cell Biol, 2015. **17**(3): p. 340-9.
57. Wang, Y., et al., *In vitro generation of colonic epithelium from primary cells guided by microstructures.* Lab Chip, 2014. **14**(9): p. 1622-31.
58. Williamson, I.A., et al., *A High-Throughput Organoid Microinjection Platform to Study Gastrointestinal Microbiota and Luminal Physiology.* Cellular and Molecular Gastroenterology and Hepatology, 2018.
59. Junick, J. and M. Blaut, *Quantification of human fecal bifidobacterium species by use of quantitative real-time PCR analysis targeting the groEL gene.* Appl Environ Microbiol. **78**(8): p. 2613-22.
60. Matsuki, T., et al., *Quantitative PCR with 16S rRNA-gene-targeted species-specific primers for analysis of human intestinal bifidobacteria.* Appl Environ Microbiol, 2004. **70**(1): p. 167-73.
61. Hermann-Bank, M.L., et al., *The Gut Microbiotassay: a high-throughput qPCR approach combinable with next generation sequencing to study gut microbial diversity.* BMC Genomics, 2013. **14**: p. 788.
62. Kwon, H.-S., et al., *Rapid identification of potentially probiotic Bifidobacterium species by multiplex PCR using species-specific primers based on the region extending from 16S rRNA through 23 S rRNA.* FEMS Microbiology Letters, 2006. **250**(1): p. 55-62.
63. Schmittgen, T.D. and K.J. Livak, *Analyzing real-time PCR data by the comparative C(T) method.* Nat Protoc, 2008. **3**(6): p. 1101-8.

64. Caporaso, J.G., et al., *QIIME allows analysis of high-throughput community sequencing data.* Nat Methods, 2010. **7**(5): p. 335-6.
65. Thompson, A.L., et al., *Milk- and solid-feeding practices and daycare attendance are associated with differences in bacterial diversity, predominant communities, and metabolic and immune function of the infant gut microbiome.* Front Cell Infect Microbiol, 2015. **5**: p. 3.
66. Devine, A.A., et al., *Impact of ileocecal resection and concomitant antibiotics on the microbiome of the murine jejunum and colon.* PLoS One, 2013. **8(8): e73140. doi:10.1371/journal.pone.0073140**.
67. Allali, I., et al., *Gut microbiome compositional and functional differences between tumor and non-tumor adjacent tissues from cohorts from the US and Spain.* Gut Microbes, 2015. **6**(3): p. 161-172.
68. Edgar, R.C., *Search and clustering orders of magnitude faster than BLAST.* Bioinformatics, 2010. **26**(19): p. 2460-1.
69. Price, M.N., P.S. Dehal, and A.P. Arkin, *FastTree 2--approximately maximum-likelihood trees for large alignments.* PLoS One, 2010. **5**(3): p. e9490.
70. Lozupone, C., M. Hamady, and R. Knight, *UniFrac--an online tool for comparing microbial community diversity in a phylogenetic context.* BMC Bioinformatics, 2006. **7**: p. 371.
71. Vieira-Silva, S., et al., *Species-function relationships shape ecological properties of the human gut microbiome.* Nat Microbiol, 2016. **1**(8): p. 16088.
72. Magnusdottir, S., et al., *Generation of genome-scale metabolic reconstructions for 773 members of the human gut microbiota.* Nat Biotechnol, 2017. **35**(1): p. 81-89.
73. Paul De Vos, e., *Bergey's Manual of Systematic Bacteriology*. 2009: Second edition. Dordrecht ; New York : Springer, [2009] ©2009.
74. Maruo, T., et al., *Adlercreutzia equolifaciens gen. nov., sp. nov., an equol-producing bacterium isolated from human faeces, and emended description of the genus Eggerthella.* Int J Syst Evol Microbiol, 2008. **58**(Pt 5): p. 1221-7.
75. Monteiro, R.A., et al., *Use of lactose to induce expression of soluble NifA protein domains of Herbaspirillum seropedicae in Escherichia coli.* Can J Microbiol, 2000. **46**(11): p. 1087-90.
76. Brooke, J.S., *Stenotrophomonas maltophilia: an emerging global opportunistic pathogen.* Clin Microbiol Rev, 2012. **25**(1): p. 2-41.
77. Kooken, J.M., K.F. Fox, and A. Fox, *Characterization of Micrococcus strains isolated from indoor air.* Mol Cell Probes, 2012. **26**(1): p. 1-5.
78. Kuete, E., et al., *Brachybacterium timonense sp. nov., a new bacterium isolated from human sputum.* New Microbes New Infect, 2019. **31**: p. 100568.
79. Duskova, D. and M. Marounek, *Fermentation of pectin and glucose, and activity of pectin-degrading enzymes in the rumen bacterium Lachnospira multiparus.* Lett Appl Microbiol, 2001. **33**(2): p. 159-63.
80. Kasperowicz, A., et al., *Sucrose phosphorylase of the rumen bacterium Pseudobutyrivibrio ruminis strain A.* J Appl Microbiol, 2009. **107**(3): p. 812-20.
81. Petzel, J.P. and P.A. Hartman, *Aromatic amino acid biosynthesis and carbohydrate catabolism in strictly anaerobic mollicutes (Anaeroplasma spp.).* Systematic and Applied Microbiology, 1990. **13**(3): p. 240-247.
82. Wallace, R.J., et al., *Eubacterium pyruvativorans sp. nov., a novel non-saccharolytic anaerobe from the rumen that ferments pyruvate and amino acids, forms caproate and utilizes acetate and propionate.* Int J Syst Evol Microbiol, 2003. **53**(Pt 4): p. 965-70.
83. Tarlera, S., et al., *Caloramator proteoclasticus sp. nov., a new moderately thermophilic anaerobic proteolytic bacterium.* Int J Syst Bacteriol, 1997. **47**(3): p. 651-6.

84. Collins, M.D., et al., *Phenotypic and phylogenetic characterization of some Globicatella-like organisms from human sources: description of Facklamia hominis gen. nov., sp. nov.* Int J Syst Bacteriol, 1997. **47**(3): p. 880-2.
85. Heyndrickx, M., et al., *Proposal of Virgibacillus proomii sp. nov. and emended description of Virgibacillus pantothenticus (Proom and Knight 1950) Heyndrickx et al. 1998.* Int J Syst Bacteriol, 1999. **49 Pt 3**: p. 1083-90.
86. Langmead, B. and S.L. Salzberg, *Fast gapped-read alignment with Bowtie 2.* Nat Methods, 2012. **9**(4): p. 357-9.
87. Abubucker, S., et al., *Metabolic reconstruction for metagenomic data and its application to the human microbiome.* PLoS Comput Biol, 2012. **8**(6): p. e1002358.
88. Shigemura, H., *Up-Regulation of MUC2 Mucin Expression by Serum Amyloid A3 Protein in Mouse.* 2014. **76**(7): p. 985-91.
89. Wlodarska, M., et al., *Antibiotic Treatment Alters the Colonic Mucus Layer and Predisposes the Host to Exacerbated Citrobacter rodentium-Induced Colitis.* Infect Immun, 2011. **79**(4): p. 1536-45.
90. Morampudi, V., et al., *The goblet cell-derived mediator RELM-beta drives spontaneous colitis in Muc2-deficient mice by promoting commensal microbial dysbiosis.* Mucosal Immunol, 2016. **9**(5): p. 1218-33.
91. Dobin, A., et al., *STAR: ultrafast universal RNA-seq aligner.* Bioinformatics, 2013. **29**(1): p. 15-21.
92. Patro, R., et al., *Salmon provides fast and bias-aware quantification of transcript expression.* Nat Methods, 2017. **14**(4): p. 417-419.
93. Love, M.I., W. Huber, and S. Anders, *Moderated estimation of fold change and dispersion for RNA-seq data with DESeq2.* Genome Biol, 2014. **15**(12): p. 550.
94. Vulevic, J., et al., *Influence of galacto-oligosaccharide mixture (B-GOS) on gut microbiota, immune parameters and metabonomics in elderly persons.* Br J Nutr, 2015. **114**(4): p. 586-95.
95. Arnold, J.W., et al., *Prebiotics for Lactose Intolerance: Variability in Galacto-Oligosaccharide Utilization by Intestinal Lactobacillus rhamnosus.* Nutrients, 2018. **10**(10).
96. Rios-Covian, D., et al., *Enhanced butyrate formation by cross-feeding between Faecalibacterium prausnitzii and Bifidobacterium adolescentis.* FEMS Microbiol Lett, 2015. **362**(21).
97. Riviere, A., et al., *Bifidobacteria and Butyrate-Producing Colon Bacteria: Importance and Strategies for Their Stimulation in the Human Gut.* Front Microbiol, 2016. **7**: p. 979.
98. Sivaprakasam, S., P.D. Prasad, and N. Singh, *Benefits of short-chain fatty acids and their receptors in inflammation and carcinogenesis.* Pharmacol Ther, 2016.
99. Lewis, K., et al., *Enhanced translocation of bacteria across metabolically stressed epithelia is reduced by butyrate.* Inflamm Bowel Dis, 2010. **16**(7): p. 1138-48.
100. Gaudier, E., et al., *Butyrate regulation of glycosylation-related gene expression: evidence for galectin-1 upregulation in human intestinal epithelial goblet cells.* Biochem Biophys Res Commun, 2004. **325**(3): p. 1044-51.
101. Renes, I.B., et al., *Epithelial proliferation, cell death, and gene expression in experimental colitis: alterations in carbonic anhydrase I, mucin MUC2, and trefoil factor 3 expression.* Int J Colorectal Dis, 2002. **17**(5): p. 317-26.
102. Aihara, E., K.A. Engevik, and M.H. Montrose, *Trefoil Factor Peptides and Gastrointestinal Function.* Annu Rev Physiol, 2017. **79**: p. 357-380.
103. Hogan, S.P., et al., *Resistin-like molecule beta regulates innate colonic function: barrier integrity and inflammation susceptibility.* J Allergy Clin Immunol, 2006. **118**(1): p. 257-68.
104. Bouchlaka, M.N., et al., *Aging predisposes to acute inflammatory induced pathology after tumor immunotherapy.* J Exp Med, 2013. **210**(11): p. 2223-37.

105. Starr, M.E., et al., *Age-Associated Increase in Cytokine Production During Systemic Inflammation-II: The Role of IL-1beta in Age-Dependent IL-6 Upregulation in Adipose Tissue.* J Gerontol A Biol Sci Med Sci, 2015. **70**(12): p. 1508-15.
106. Laaf, D., et al., *Galectin-Carbohydrate Interactions in Biomedicine and Biotechnology.* Trends Biotechnol, 2019. **37**(4): p. 402-415.
107. Jones, R.M. and A.S. Neish, *Redox signaling mediated by the gut microbiota.* Free Radic Biol Med, 2017. **105**: p. 41-47.
108. Clapham, D.E., L.W. Runnels, and C. Strubing, *The TRP ion channel family.* Nat Rev Neurosci, 2001. **2**(6): p. 387-96.
109. Williamson, I.T., et al., *A high-throughput organoid microinjection platform to study gastrointestinal microbiota and luminal physiology.* Cellular and Molecular Gastroenterology and Hepatology, 2018. **In press.**
110. Shoaf, K., et al., *Prebiotic galactooligosaccharides reduce adherence of enteropathogenic Escherichia coli to tissue culture cells.* Infection and Immunity, 2006. **74**(12): p. 6920-28.
111. Zhao, S., et al., *Akkermansia muciniphila improves metabolic profiles by reducing inflammation in chow diet-fed mice.* J Mol Endocrinol, 2017. **58**(1): p. 1-14.
112. Collado, M.C., et al., *Intestinal integrity and Akkermansia muciniphila, a mucin-degrading member of the intestinal microbiota present in infants, adults, and the elderly.* Appl Environ Microbiol, 2007. **73**(23): p. 7767-70.
113. Nicoletti, C., *Age-associated changes of the intestinal epithelial barrier: local and systemic implications.* Expert Rev Gastroenterol Hepatol, 2015. **9**(12): p. 1467-9.
114. Zwielehner, J., et al., *Combined PCR-DGGE fingerprinting and quantitative-PCR indicates shifts in fecal population sizes and diversity of Bacteroides, bifidobacteria and Clostridium cluster IV in institutionalized elderly.* Exp Gerontol, 2009. **44**(6-7): p. 440-6.
115. Raul, F., et al., *Age related increase of brush border enzyme activities along the small intestine.* Gut, 1988. **29**(11): p. 1557-63.
116. Lee, M.F., et al., *Total intestinal lactase and sucrase activities are reduced in aged rats.* J Nutr, 1997. **127**(7): p. 1382-7.
117. Matsuki, T., et al., *Infant formula with galacto-oligosaccharides (OM55N) stimulates the growth of indigenous bifidobacteria in healthy term infants.* Benef Microbes, 2016. **7**(4): p. 453-61.
118. So, D., et al., *Dietary fiber intervention on gut microbiota composition in healthy adults: a systematic review and meta-analysis.* Am J Clin Nutr, 2018. **107**(6): p. 965-983.
119. Szklany, K., et al., *Supplementation of dietary non-digestible oligosaccharides from birth onwards improve social and reduce anxiety-like behaviour in male BALB/c mice.* Nutr Neurosci, 2019: p. 1-15.
120. Cheng, W., et al., *Effect of Functional Oligosaccharides and Ordinary Dietary Fiber on Intestinal Microbiota Diversity.* Front Microbiol, 2017. **8**: p. 1750.
121. Zimmermann, P. and N. Curtis, *The effect of antibiotics on the composition of the intestinal microbiota - a systematic review.* J Infect, 2019. **79**(6): p. 471-489.
122. Barbut, F. and J.L. Meynard, *Managing antibiotic associated diarrhoea.* BMJ, 2002. **324**(7350): p. 1345-6.
123. Ladirat, S.E., et al., *Impact of galacto-oligosaccharides on the gut microbiota composition and metabolic activity upon antibiotic treatment during in vitro fermentation.* FEMS Microbiol Ecol, 2014. **87**(1): p. 41-51.
124. Ríos-Covián, D., et al., *Intestinal Short Chain Fatty Acids and their Link with Diet and Human Health.* Front Microbiol, 2016. **7**.
125. den Besten, G., et al., *The role of short-chain fatty acids in the interplay between diet, gut microbiota, and host energy metabolism.* J Lipid Res, 2013. **54**(9): p. 2325-40.

126. D'Souza, W.N., et al., *Differing roles for short chain fatty acids and GPR43 agonism in the regulation of intestinal barrier function and immune responses.* PLoS One, 2017. **12**(7): p. e0180190.
127. Tan, J., et al., *The role of short-chain fatty acids in health and disease.* Adv Immunol, 2014. **121**: p. 91-119.
128. Mitra, S.K., D.A. Hanson, and D.D. Schlaepfer, *Focal adhesion kinase: in command and control of cell motility.* Nat Rev Mol Cell Biol, 2005. **6**(1): p. 56-68.
129. Petit, V. and J.P. Thiery, *Focal adhesions: structure and dynamics.* Biol Cell, 2000. **92**(7): p. 477-94.
130. Kudryavtseva, A.V., et al., *Mitochondrial dysfunction and oxidative stress in aging and cancer.* Oncotarget, 2016. **7**(29): p. 44879-44905.
131. Vartak, R., C.A. Porras, and Y. Bai, *Respiratory supercomplexes: structure, function and assembly.* Protein Cell, 2013. **4**(8): p. 582-90.
132. Arnold, J.W., J. Roach, and M.A. Azcarate-Peril, *Emerging technologies for gut microbiome research.* Trends in microbiology, 2016. **24**(11): p. 887-901.
133. Tran, L. and B. Greenwood-Van Meerveld, *Age-associated remodeling of the intestinal epithelial barrier.* J Gerontol A Biol Sci Med Sci, 2013. **68**(9): p. 1045-56.
134. Mitchell, E.L., et al., *Reduced Intestinal Motility, Mucosal Barrier Function, and Inflammation in Aged Monkeys.* J Nutr Health Aging, 2017. **21**(4): p. 354-361.
135. Szklarczyk, D., et al., *STRING v11: protein-protein association networks with increased coverage, supporting functional discovery in genome-wide experimental datasets.* Nucleic Acids Res, 2019. **47**(D1): p. D607-D613.
136. Metsalu, T. and J. Vilo, *ClustVis: a web tool for visualizing clustering of multivariate data using Principal Component Analysis and heatmap.* Nucleic Acids Res, 2015. **43**(W1): p. W566-70.

Figure Legends

Figure 1: The aging gut has a distinct microbiome (a) Phylogenetic diversity and species richness in stool samples from old (n=12) and young mice (n=12), **(b)** Unweighted Unifrac Principal Coordinate Analysis (PCoA) plot of samples, **(c)** Relative abundance of saccharolytic, non-saccharolytic and unclassified bacteria by age, **(d)** Comparative analysis of differences in abundance of specific genera between young and old animals.

Figure 2: Prebiotic GOS and antibiotics decrease microbiome diversity in the gut. GOS increase the abundance of prebiotic-metabolizing enzymes (a) Experimental design outlining timepoints T1 (post standardization), T2 (post specialized diet), T3 (post antibiotics in water), T4 (post clindamycin IP injection), and T5 (pre-sacrifice) (N=48) **(b)** Impact of the different treatments on phylogenetic diversity. GOS reduced diversity in both old and young animals. Diversity recovered at T3 but declined again at T4 after IP clindamycin, **(c)** Relative abundance of saccharolytic, non-saccharolytic, and bacteria of undetermined metabolism over time. Line colors are as in 2b, **(d)** Whole Genome Shotgun (WGS) sequencing of selected stool samples showed that GOS treatment increased the abundance of beta-glucosidases/cellobioses of the GH1 family of glycosyl hydrolases, and beta-galactosidases of the GH1, Gh2, and GH42 families. These enzymes are essential to metabolize GOS in the gut.

Figure 3: Unweighted Unifrac PCoA plots and differences in relative abundance of specific bacteria at different timepoints and treatments (a) The T1-T2 PCoA plot (Left) revealed baseline differences between old and young mice and how GOS induced a convergence of young and old samples in Cluster 3 (OC=old mice, control diet, OG= old mice, GOS diet, YC=young mice, control diet, YG=young mice, GOS diet). The middle panel shows the prebiotic impact on young (dark purple) and old (red) mice compared to the control diet (light purple = young control, light pink = old control). The right panel shows composed differences in

relative abundances by age, diet and time point. **(b)** The T2-T3 PCoA plot (left) and genus-level analysis (middle) showed a minor impact of the antibiotic treatment in water. Middle panel: Control and GOS diets as before. Light blue dots represent no antibiotic treatment, dark blue represent antibiotic treatment. **(c)** The T3-T4 PCoA plot (left) and genus-level analysis (middle) represent samples immediately after clindamycin IP injection. The graphs did not show dramatic impacts to the microbiome, which were clearly visible in **(d)** the T4-T5 PCoA and taxa plots. At this timepoint transition a new cluster (Cluster 5), which encompass only antibiotic-treated control animals, was observed.

Figure 4: (a) Old mice had higher intestinal permeability measured by FITC-dextran assays than young animals. Intestinal permeability was reduced in GOS fed mice (i) via increased expression of *MUC2*. Expression of TFF3 and RELMb tended to increase in the GOS groups but differences were not statistically significant (ii). Paraformaldehyde vapor fixation and subsequent PAS staining showed increased mucus thickness in old mice fed the prebiotics diet (iii). **(b) Inflammatory biomarkers were modulated by GOS and antibiotics**. A 2 x 2 x 2 ANOVA showed increased serum IL-6 and IL-17 in antibiotic treated mice regardless of age or diet (i). Similarly, serum IL-13 was higher in young mice regardless of diet or antibiotics (ii). Eotaxin (iii) and IP-10 (iv) were higher in the GOS group within the no-antibiotic animals but lower in the GOS group that received antibiotics regardless of age. No significant differences in serum IL-6 were observed by age or diet in the no-antibiotics group. Within the animals that received antibiotics, old mice had a non-significant increased concentration of the cytokine while mice on the GOS diet had higher levels of IL-6 regardless of age (v). Finally, expression of TNFα quantified by RT-qPCR was higher in old animals compared to young and reduced by GOS treatment in old animals.

Figure 5: STRING network analysis [135] of expression data from colon showed different GOS effects on the intestinal epithelium of old and young mice. (a) GOS induced expression of binding-related genes (GO:0005488) in young mice while inducing **(b)** small molecule metabolic processes genes (GO:0044281) in old animals. Network nodes represent predicted proteins. Splice isoforms or post-translational modifications are collapsed so each node represents all the proteins produced by a single, protein-coding gene locus. The confidence cutoff for showing interaction links was 0.900 (highest). The lower panel in figure (a) shows the most represented GO categories within binding-related genes in our transcriptomics data. **(c) A heatmap of expression data revealed that GOS act as a modulator of the immune system in old and young mice.** The heatmap was generated using ClustVis [136]. Rows were centered; unit variance scaling was applied to rows. Rows were clustered using correlation distance and average linkage.

Figure 6: (a) Top figure: The variable bifidogenic effect observed *in vivo* was reproduced *in vitro* in the organoid platform (data from 16S rRNA amplicon sequencing). Bottom figure: The genus *Bifidobacterium* was quantified by high throughput qPCR in stools from mice and organoid contents. **(b)** Shannon diversity and species richness within microbiota-colonized organoids declined over time. The continuous lines represent data from organoids injected with stools from young mice. Dash lines are results from organoids injected with stools from old mice. **(c)** Unweighted Unifrac PCoA plots revealed differences between old and young microbiota upon colonization in organoids, which converged to a single grouping over 72-hours. **(e)** Taxonomy plots of microbiota-colonized organoids showed changes over time in communities derived from both old and young animals.

Figure S1: Relative abundance of *Bacteroides* (a), *Akkermansia muciniphila* (b), and *Lactobacillus* (c) were increased by GOS diets. Abundance of *Clostridium* (d), *Adlecreutzia* (e) and *Ruminococcus* (f) were reduced by GOS diets.

Figure S2: Effect of antibiotics on abundance of specific bacterial taxa in young and old animals.

Figure S3: Heatmap represents changes in bacterial abundance within old microbiota-colonized organoids over time when supplemented with either PBS (control), GOS, or Lactose.

Figure S4: Heatmap represents changes in bacterial abundance within young microbiota-colonized organoids over time when supplemented with either PBS (control), GOS, or Lactose.

Figures

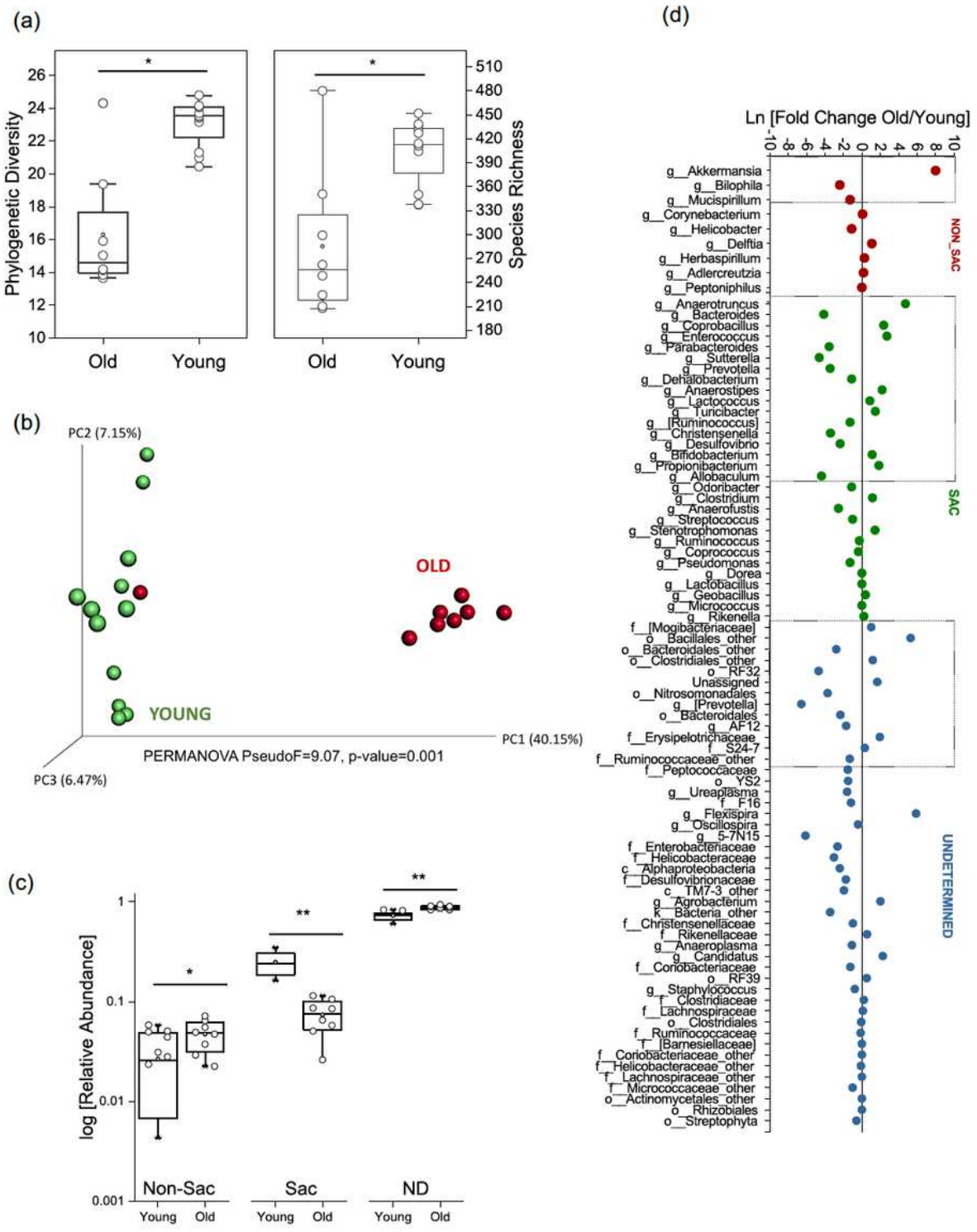

Figure 1

The aging gut has a distinct microbiome (a) Phylogenetic diversity and species richness in stool samples from old (n=12) and young mice (n=12), (b) Unweighted Unifrac Principal Coordinate Analysis (PCoA) plot of samples, (c) Relative abundance of saccharolytic, non-saccharolytic and unclassified bacteria by

age, (d) Comparative analysis of differences in abundance of specific genera between young and old animals.

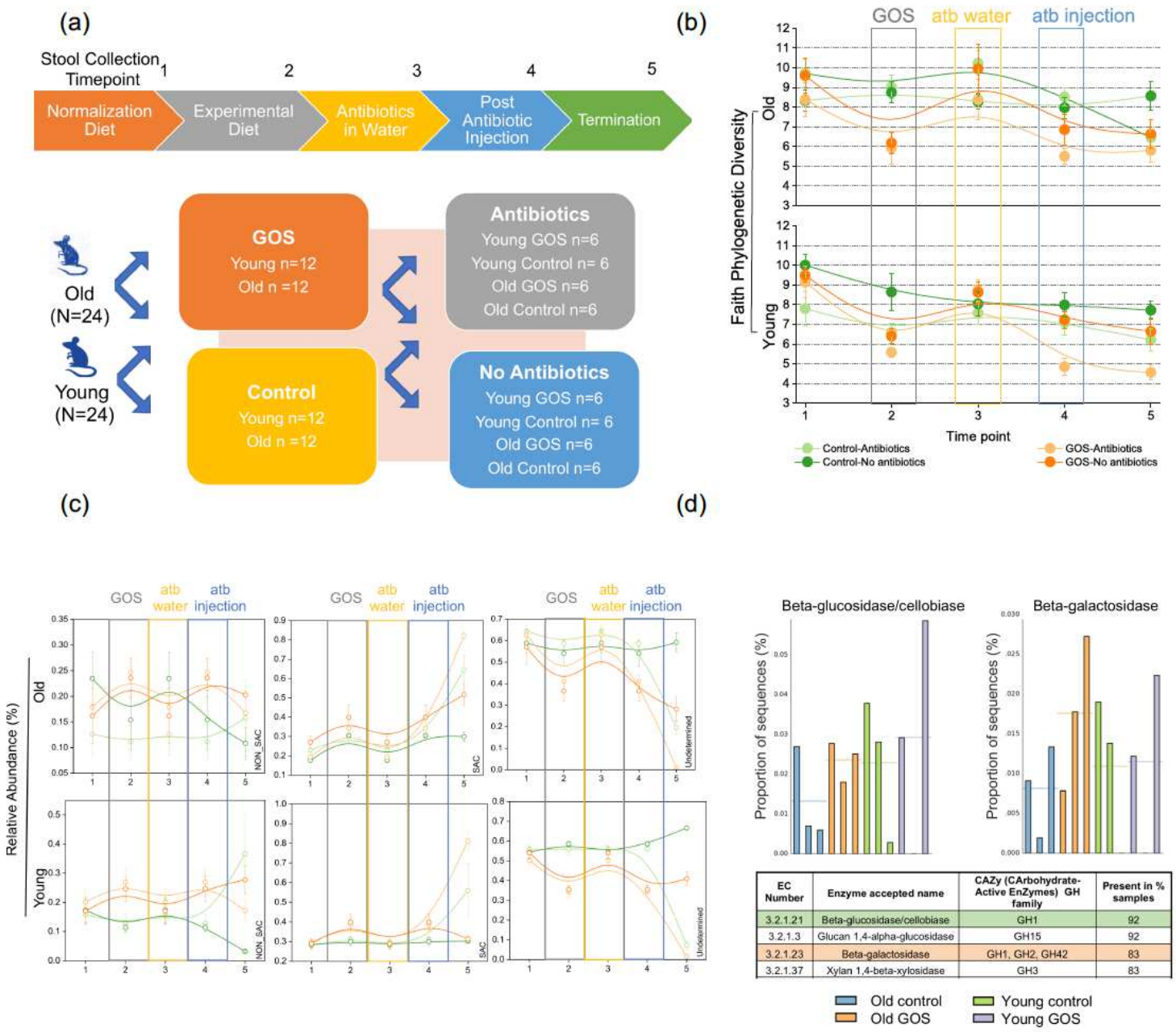

EC Number	Enzyme accepted name	CAZy (CArbohydrate-Active EnZymes) GH family	Present in % samples
3.2.1.21	Beta-glucosidase/cellobiase	GH1	92
3.2.1.3	Glucan 1,4-alpha-glucosidase	GH15	92
3.2.1.23	Beta-galactosidase	GH1, GH2, GH42	83
3.2.1.37	Xylan 1,4-beta-xylosidase	GH3	83

Figure 2

Prebiotic GOS and antibiotics decrease microbiome diversity in the gut. GOS increase the abundance of prebiotic-metabolizing enzymes (a) Experimental design outlining timepoints T1 (post standardization), T2 (post specialized diet), T3 (post antibiotics in water), T4 (post clindamycin IP injection), and T5 (pre-sacrifice) (N=48) (b) Impact of the different treatments on phylogenetic diversity. GOS reduced diversity in both old and young animals. Diversity recovered at T3 but declined again at T4 after IP clindamycin, (c) Relative abundance of saccharolytic, non-saccharolytic, and bacteria of undetermined metabolism over time. Line colors are as in 2b, (d) Whole Genome Shotgun (WGS) sequencing of selected stool samples showed that GOS treatment increased the abundance of betaglucosidases/ cellobioses of the GH1 family

of glycosyl hydrolases, and beta-galactosidases of the GH1, Gh2, and GH42 families. These enzymes are essential to metabolize GOS in the gut.

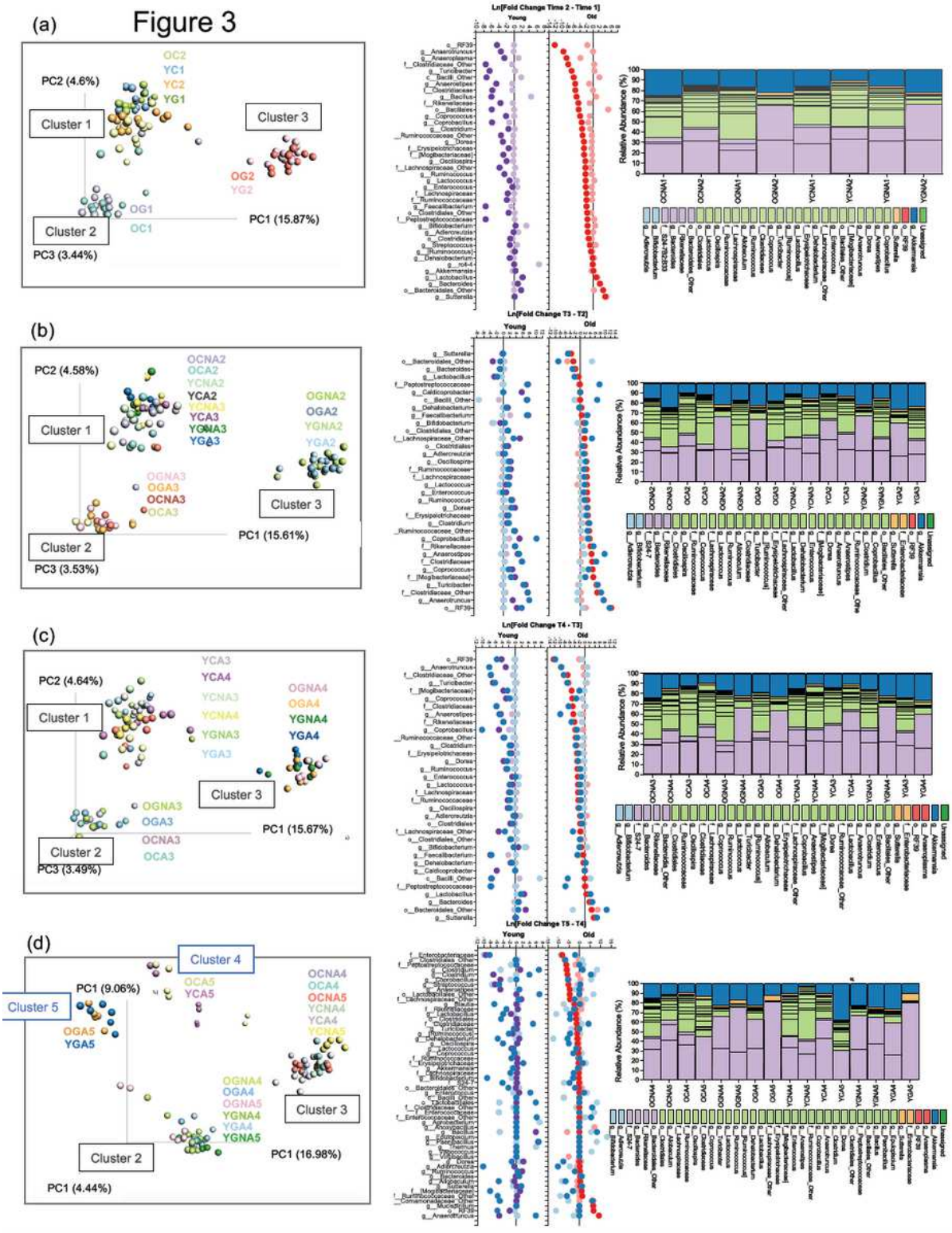

Figure 3

Unweighted Unifrac PCoA plots and differences in relative abundance of specific bacteria at different timepoints and treatments (a) The T1-T2 PCoA plot (Left) revealed baseline differences between old and young mice and how GOS induced a convergence of young and old samples in Cluster 3 (OC=old mice,

control diet, OG= old mice, GOS diet, YC=young mice, control diet, YG=young mice, GOS diet). The middle panel shows the prebiotic impact on young (dark purple) and old (red) mice compared to the control diet (light purple = young control, light pink = old control). The right panel shows composed differences in relative abundances by age, diet and time point. (b) The T2-T3 PCoA plot (left) and genus-level analysis (middle) showed a minor impact of the antibiotic treatment in water. Middle panel: Control and GOS diets as before. Light blue dots represent no antibiotic treatment, dark blue represent antibiotic treatment. (c) The T3-T4 PCoA plot (left) and genus-level analysis (middle) represent samples immediately after clindamycin IP injection. The graphs did not show dramatic impacts to the microbiome, which were clearly visible in (d) the T4-T5 PCoA and taxa plots. At this timepoint transition a new cluster (Cluster 5), which encompass only antibiotic-treated control animals, was observed.

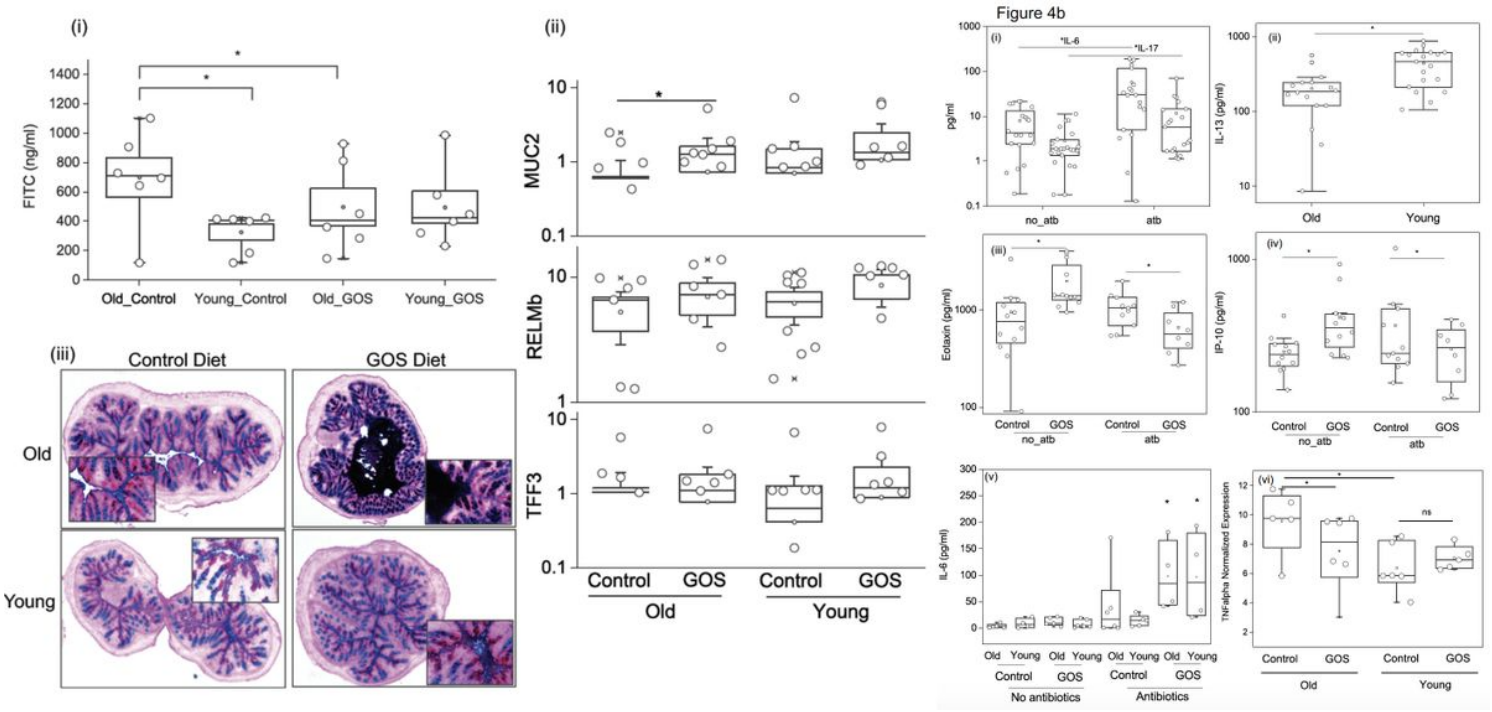

Figure 4

(a) Old mice had higher intestinal permeability measured by FITC-dextran assays than young animals. Intestinal permeability was reduced in GOS fed mice (i) via increased expression of MUC2. Expression of TFF3 and RELMb tended to increase in the GOS groups but differences were not statistically significant (ii). Paraformaldehyde vapor fixation and subsequent PAS staining showed increased mucus thickness in old mice fed the prebiotics diet (iii). (b) Inflammatory biomarkers were modulated by GOS and antibiotics. A 2 x 2 x 2 ANOVA showed increased serum IL-6 and IL-17 in antibiotic treated mice regardless of age or diet (i). Similarly, serum IL-13 was higher in young mice regardless of diet or antibiotics (ii). Eotaxin (iii) and IP-10 (iv) were higher in the GOS group within the no-antibiotic animals but lower in the GOS group that received antibiotics regardless of age. No significant differences in serum IL-6 were observed by age or diet in the no-antibiotics group. Within the animals that received antibiotics, old mice had a non-significant increased concentration of the cytokine while mice on the GOS diet had higher levels of IL-6

regardless of age (v). Finally, expression of TNFa quantified by RT-qPCR was higher in old animals compared to young and reduced by GOS treatment in old animals.

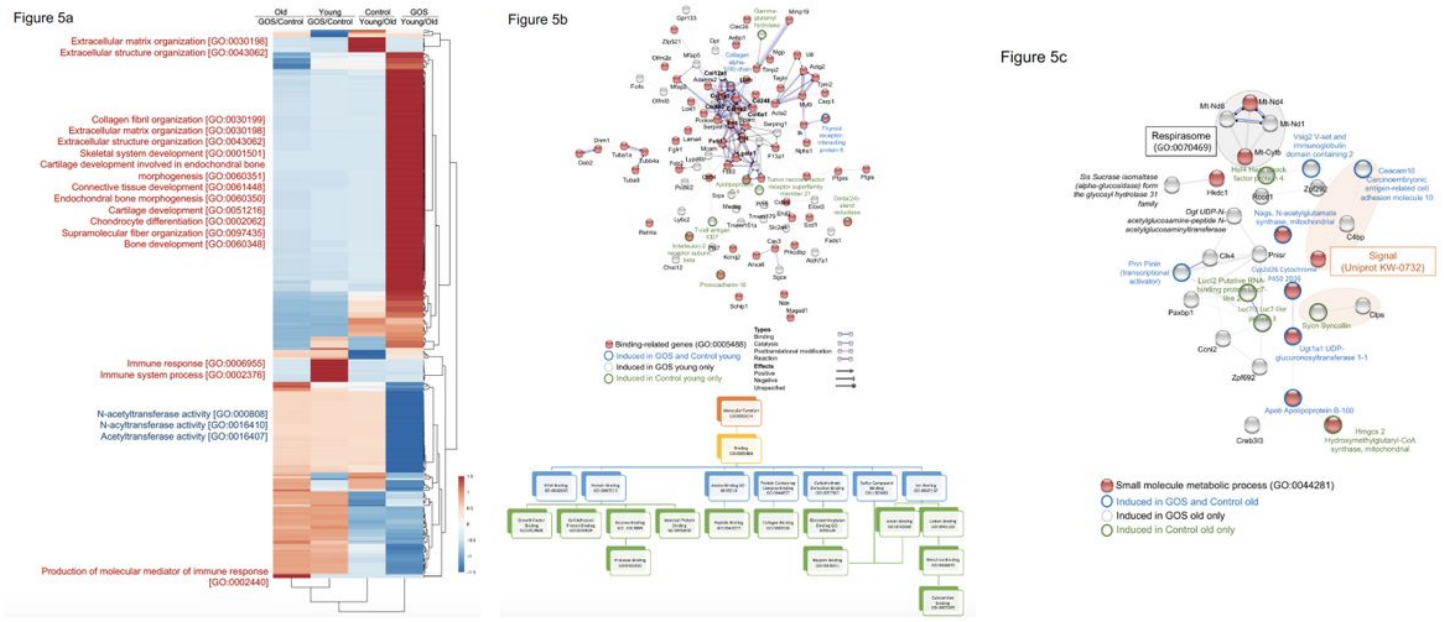

Figure 5

STRING network analysis [135] of expression data from colon showed different GOS effects on the intestinal epithelium of old and young mice. (a) GOS induced expression of binding-related genes (GO:0005488) in young mice while inducing (b) small molecule metabolic processes genes (GO:0044281) in old animals. Network nodes represent predicted proteins. Splice isoforms or post-translational modifications are collapsed so each node represents all the proteins produced by a single, protein-coding gene locus. The confidence cutoff for showing interaction links was 0.900 (highest). The lower panel in figure (a) shows the most represented GO categories within binding-related genes in our transcriptomics data. (c) A heatmap of expression data revealed that GOS act as a modulator of the immune system in old and young mice. The heatmap was generated using ClustVis [136]. Rows were centered; unit variance scaling was applied to rows. Rows were clustered using correlation distance and average linkage.

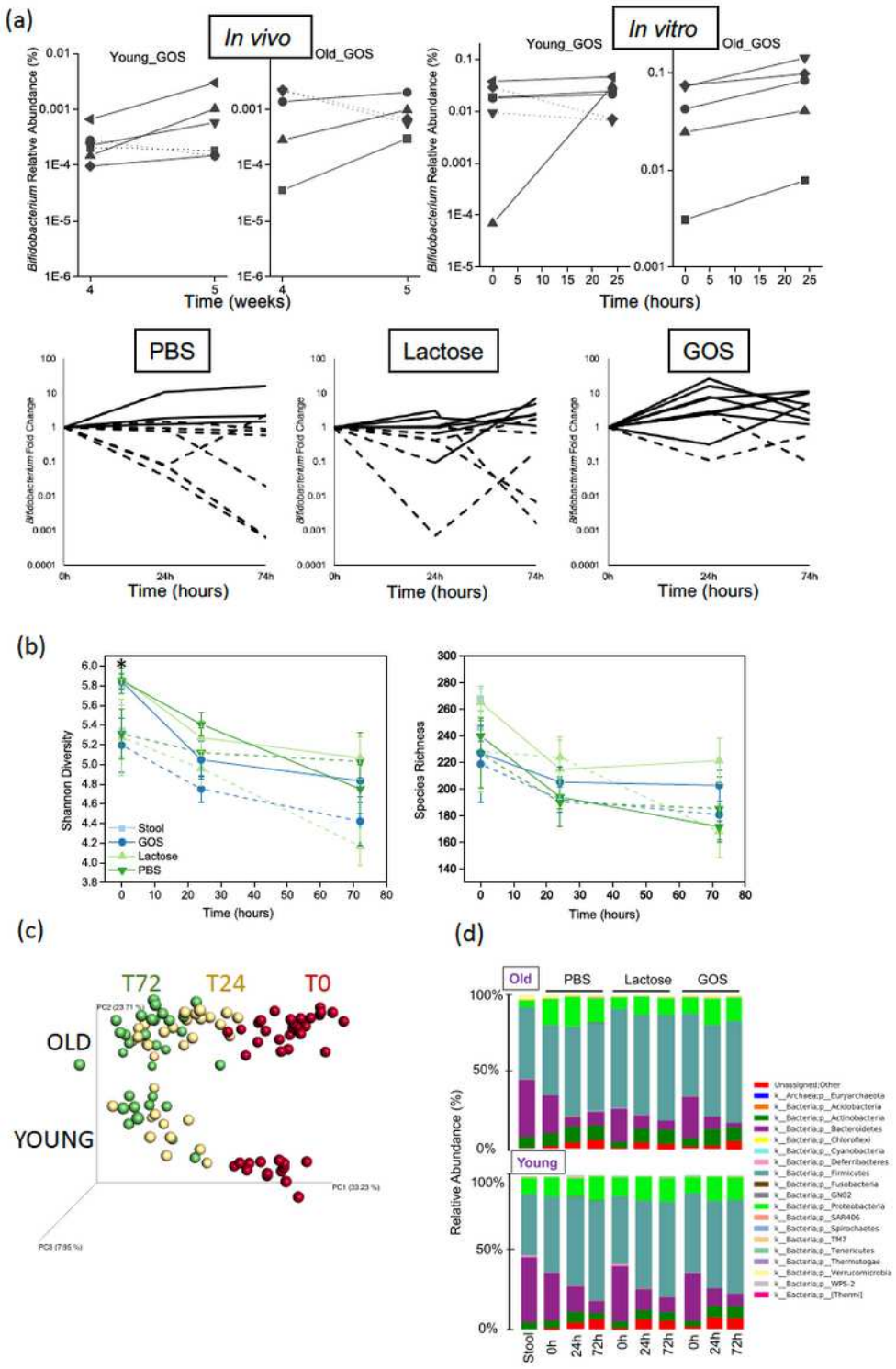

Figure 6

(a) Top figure: The variable bifidogenic effect observed in vivo was reproduced in vitro in the organoid platform (data from 16S rRNA amplicon sequencing). Bottom figure: The genus Bifidobacterium was quantified by high throughput qPCR in stools from mice and organoid contents. (b) Shannon diversity and species richness within microbiota-colonized organoids declined over time. The continuous lines represent data from organoids injected with stools from young mice. Dash lines are results from

organoids injected with stools from old mice. (c) Unweighted Unifrac PCoA plots revealed differences between old and young microbiota upon colonization in organoids, which converged to a single grouping over 72-hours. (e) Taxonomy plots of microbiota-colonized organoids showed changes over time in communities derived from both old and young animals.

Supplementary Files

This is a list of supplementary files associated with this preprint. Click to download.

- SupplementaryText.pdf
- SupplementalFigures.pdf
- SupplementaryTable1.pdf
- SupplementaryTable2.xlsx